Impact of Hurricane Irma on Coral Reef Sediment Redistribution at Looe Key Reef, Florida, USA

Kimberly K. Yates[1], Zachery Fehr[2], Selena Johnson[1], David Zawada[1]

[1]U.S. Geological Survey, St. Petersburg, FL, 33701, United States

5   [2]Cherokee Nation System Solutions, Tulsa, OK, 74166, United States, Contractor to the U.S. Geological Survey

Correspondence to: Kimberly K. Yates (kyates@usgs.gov)

Abstract. Understanding event-driven sediment transport in coral reef environments is essential to assessing impacts to reef species, habitats, restoration, and mitigation, yet there remains a global knowledge gap due to limited quantitative studies. Hurricane Irma made landfall in the Lower Florida Keys with sustained 209 km h^{-1} winds and greater than 8 m waves on 10

10 September 2017, directly impacting the Florida Reef Tract (FRT), and providing an opportunity to perform a unique comprehensive, quantitative assessment of its impact on coral reef structure and sediment redistribution. We used lidar and multibeam derived digital elevation models (DEMs) collected before and after the passing of Hurricane Irma over a 15.98 km^2 area along the Lower FRT including Looe Key Reef to quantify changes in seafloor elevation, volume, and structure due to storm impacts. Elevation change was calculated at over 4-million point-locations across 10 habitat types within this study area

15 for two time periods using data collected from 1) approximately one year before the passing of Irma and three to six months following the storm's impact, and 2) from three to six months after, and up to 16.5 months after, the storm. Elevation-change data were then used to generate Triangulated Irregular Network (TIN) models in ArcMap to calculate changes in seafloor volume during each time-period. Our results indicate that Hurricane Irma was primarily a depositional event that increased mean seafloor elevation and volume at this study site by 0.34 m and up to 5.4 Mm^3, respectively. Sediment was transported

20 primarily west-southwest (WSW) and downslope modifying geomorphic seafloor features including the migration of sand waves and rubble fields, formation of scour marks in shallow seagrass habitat, and burial of seagrass and coral-dominated habitat. Approximately 16.5 months after Hurricane Irma (during a 13-month period between 2017 and 2019), net erosion was observed across all habitats with mean elevation-change of -0.15 m and net volume change up to -2.46 Mm^3. Rates of elevation change during this post-storm period were one to two orders of magnitude greater than decadal and multi-decadal rates of

25 change in the same location, and changes showed erosion of approximately 50% of sediment deposited during the storm event as seafloor sediment distribution began to re-equilibrate to non-storm sea state conditions. Our results suggest higher resolution elevation-change data collected over seasonal and annual time periods could enhance characterization and understanding of short-term and long-term rates and processes of seafloor change.

1 Introduction

30 Coral reefs provide a variety of services to coastal communities including protection from coastal hazards such as storms, waves, and erosion (Ferrario et al., 2014; Storlazzi et al., 2021); socioeconomic benefits such as fisheries, recreation, and tourism (Moberg and Folk, 1999; Hall et al., 2020); and they support numerous habitats and diverse marine species (Knowlton, 2020). Socioeconomic benefits of Florida reefs have an estimated value of over eight billion dollars a year, supporting 39,000 South Florida jobs and 70,400 total jobs, with at least 2.9 billion dollars contributing directly to the local economy (Krediet et

35 al., 2009; Gorstein et al., 2016, Towle et al., 2020). Benthic communities of the Florida Reef Tract (FRT) have been degrading for the past several decades. Coral coverage has declined across the Caribbean and Florida reefs by more than 50% since the 1970's due to coral disease and bleaching (Porter et al., 2001; Patterson et al., 2002; Williams and Miller, 2012; Joyner et al., 2015; Walker et al., 2018), pollution and overfishing (Littler et al., 1986; Lapointe & Clark, 1992; and Hughes 1994), and mass-mortality of macroalgal grazers (e.g., Lessios et al., 1983). Progression of climate change has increased thermal stress,

40 coral bleaching and disease, ocean acidification, and corallivory (predation of corals) (Wilkinson 1996; Mumby et al., 2006; Brandt and McManus, 2009; Soto et al., 2011; Kuffner et al., 2015; Randall and van Woesik, 2015; Muehllehner et al., 2016; Hughes et al., 2017; Rice et al., 2019). These multiple stressors and increased storm occurrences have caused a shift from stony-coral-dominated reefs to macroalgae and octocoral dominated reefs (Bohsnack 1983; Hughs, 1994; Knowlton, 1992; Miller et al., 2002; Norstrom et al., 2009; Bruno et al., 2009; Ruzicka et al., 2013 and Jackson et al., 2014). Coral coverage

45 has been reported at less than 7% along the Florida Keys Reef Tract and less than 3% along the northern FRT in recent years (Jackson et al., 2014; Walton et al, 2018; Knowlton, 2020); and many of Florida's reefs are in a net erosional state (Yates et al., 2017; Morris et al., 2022). Additionally, seagrass has been decreasing in coverage since early *Thalassia testudinum* die-offs in 1987 following decreased water quality and phytoplankton blooms during the previous decade and more contemporary die-offs in 2015 following storm events and water quality variations (Hall et al., 2016; Krause et al., 2023). Analysis of 25

50 years of benthic monitoring data (from 1995 to 2020) from South Florida including the FKNMS by Krause et al. (2023) showed primarily long-term stability of seagrass meadows over this period with species composition transitions from dense *T. testudinum* meadows toward mixed communities including macroalgae in locations with higher nutrient inputs. However, their results also showed instantaneous seagrass loss due to storm-related physical disturbance at over 10% of monitoring sites including near the FRT likely due to wave-induced erosion during major storm events, and none of these sites showed full

55 revegetation with seagrass over the 25-yr monitoring period.

Multi-decadal seafloor elevation-change analyses along the FRT indicate that degradation of coral reefs and surrounding seafloor habitats has led to substantial erosion and loss of elevation from the 1930's to 2002 and increased water depths to levels not expected until near the year 2100 (Yates et al., 2017). Continued FRT coral reef degradation and loss of seafloor

60 elevation is projected to increase flooding risk from storms and coastal inundation to more than 7,300 people and to cause $823.6 million in direct and indirect damage to housing, buildings, and businesses, annually (Storlazzi et al., 2021, estimated

in 2010 U.S. dollars, USD). Storm frequency and strength are projected to increase as sea-surface temperatures and atmospheric energy increase due to climate change and global warming (Elsner et al., 2008, Bhatia et al., 2019; Knutson et al., 2020). While advances have been made in understanding long-term change in seafloor elevation and structure and its potential
65   socioeconomic consequences, understanding the effects of event-driven changes to seafloor geomorphology due to storms remains a major knowledge gap.

Major tropical storms persistently impact the state of Florida with historical hurricane impacts estimated to have caused more than $450 billion dollars of damage across the state from the early 1900's to 2007 (Malmstadt et al., 2009). The Middle to
70   Lower Florida Keys (from Islamorada to Key West) has been impacted by 15 major hurricane landfall events (Category 3 through 5) and numerous tropical storm and Category 1 and 2 hurricanes from the early 1900's to 2022 (NOAA, 2022a). Hurricane Irma made landfall at Cudjoe Key in the Lower Florida Keys after passing directly over Looe Key Reef on 10 September 2017 as a category 4 hurricane with maximum wind speeds of 213 km h^{-1} (115 kts) (Cangialosi et al., 2021) and significant wave heights of approximately 14 m a few kilometers offshore of the Florida Keys (Xian et al., 2018, Fig. 1a, b).
75   Satellite imagery showed extensive sediment plumes throughout South Florida and the FRT caused by sediment resuspension and transport during the storm (Fig. 1c, d). The storm damaged up to 75% of buildings near its landfall point and caused approximately 50 billion USD of wind and water damage across the state of Florida (Xian et al., 2018; Cangialosi et al., 2021; NOAA, 2022b). Prior to Hurricane Irma, the most recent, direct impact to Looe Key Reef from a tropical storm was in 2008 during Tropical Storm Fay (NOAA, 2022a).

80

Numerous rapid assessments of seafloor habitats were conducted along the FRT in the weeks following Hurricane Irma. Diver-based surveys of coral reefs at 57 locations along the FRT by the National Oceanic and Atmospheric Administration showed highest levels of damage in the Middle to Lower Keys including dislodged and fractured corals, clogged and damaged sponges, heavy sedimentation, burial of corals, displaced rubble and sand, reef erosion, fractured substrate, and marine debris; 14% of
85   sites showed severe impact, 33% showed moderate impact, and 53% showed minimal impact (Viehman et al., 2018). Looe Key Reef, located near the hurricane landfall location, showed more than 26% prevalence of hurricane-impacted corals (Florida Resilience Program, 2017). Similar surveys along the northern FRT from Key Biscayne north showed from approximately 5% to 17% of 62 sites with impacts to corals including dislodged and buried colonies, and at least one site with slabs of hardbottom 2 to 5 m in size fractured and displaced several meters (Walker, 2018). Analyses of long-term monitoring-transect data at 40
90   sites throughout the Florida Keys National Marine Sanctuary (FKNMS) showed instantaneous losses in seagrass and calcareous green macroalgae density after the storm passed, particularly in the Lower Florida Keys near where Hurricane Irma made landfall (Wilson et al., 2020). Additionally, several locations showed moderate burial of seagrass with up to 5 to 10 cm of sand, while other locations showed heavy erosion or moderate seagrass canopy thinning (Wilson et al., 2020). Reef Visual Census (RVC) surveys including structure from motion (SfM) habitat photogrammetry at sites in the Lower Florida Keys from
95   February 2017 to December 2018 showed a 30% decrease in macroalgae at the Looe Key Sanctuary Preservation Area (SPA)

and a 30% increase at the Looe Key Special Use Area (SPU) post Irma; while both Looe Key locations showed a 10% decrease in live coral cover and a 20% increase in octocoral cover (Simmons et al., 2022). Comparison of restored (outplant) coral survival rates at two fore reef and two patch reef sites near Tavernier Key in the Upper Florida Keys showed approximately 85% outplant survival at all locations prior to the passage of Hurricane Irma; however, no outplants survived at the fore reef sites and only 51% of outplants survived at the patch reef sites post-Irma, the difference likely due to protection of the patch reefs from dissipation of wave energy by the reef crest (Lohr et al., 2020). Examination of *Diadema antillarum* sea urchins (a

key reef grazer) density, size structure, and coral reef community structure before and 2.5 months after Irma at 10 locations in the Middle and Upper Florida Keys showed a significant decrease in *D. antillarum* density with increased sedimentation, suggesting sediment transport caused mortality through abrasion and burial (Kobelt et al., 2019).

While observational data from several locations indicate seafloor sediments were transported and likely caused damage to benthic habitats, the direct impact of Hurricane Irma or other tropical storms on seafloor elevation and geomorphologic structures has not previously been quantified along the FRT. In this study, we used high-resolution light-detection-and-ranging (lidar) and multibeam bathymetry data collected before and after the passage of Hurricane Irma to quantify seafloor elevation and volume change of benthic habitats and geomorphological structures resulting from the storm's impact and post-storm re-equilibration of seafloor sediments at more than 4-million point-locations at the Looe Key Reef system in the Lower FRT.

2 Materials and methods

2.1 Looe Key Reef Study Site

The FRT is the only living coral shelf reef in the continental United States, and it spans more than 580 km along the east coast of Florida from St. Lucie Inlet to the Dry Tortugas, with total reef area of approximately 1,179 km^2 (Lidz et al., 2003; Finkl and Andrews, 2008; Jackson et al., 2014; Florida Department of Environmental Protection, 2022). Water depth along the FRT is up to approximately 20 m with discontinuous spur and groove formations and patch reefs separated by tidal passes, and it is characterized by both coral-dominated and non-coral dominated seafloor habitat as characterized and mapped by the Florida Fish and Wildlife Conservation Commission-Fish and Wildlife Research Institute (FWC, 2015). Much of the FRT is protected by the FKNMS, Biscayne National Park, and Dry Tortugas National Park, and includes several sanctuary preservation areas (SPAs) and special use areas (SPUs) within FKNMS, including the Looe Key SPA and SPU, that together protect over 6000 marine species (Keller and Donahue, 2006). Looe Key Reef is a barrier bank reef located approximately 10 km offshore in the Lower Florida Keys, south of Cudjoe Key, and it is characterized by a prominent, shallow reef crest with two extensive coral rubble fields, a fore reef with a spur-and-groove formation, a forereef terrace and deep reef zone, and a back reef area with seagrass communities, patch reefs, and individual coral heads (Fig. 2a-d). Seagrass beds and sandflats with intermittent patch reefs extend shoreward from Looe Key Reef proper to Hawk Channel, approximately 2 km to the north. Looe Key SPA, located at approximately 24° 32' N, 81° 24' W, is just over 18 km^2 and surrounds LKR proper which is less than 1.7 km^2. Looe

Key Reef contains a coral nursery and several restoration sites for coral outplants; it is one of seven FKNMS iconic reefs, and
140 the focus of a major collaborative habitat restoration effort known as Mission: Iconic reefs (NOAA Fisheries, 2022).

The northeastern eyewall of Hurricane Irma passed directly over LKR with the storm's center passing approximately 9 km
west of LKR. However, the storm was approximately 684 km in diameter and covered the entire FRT and much of South
Florida. The National Weather Service's technical summary of the storm reported tropical storm force winds more than 640

145
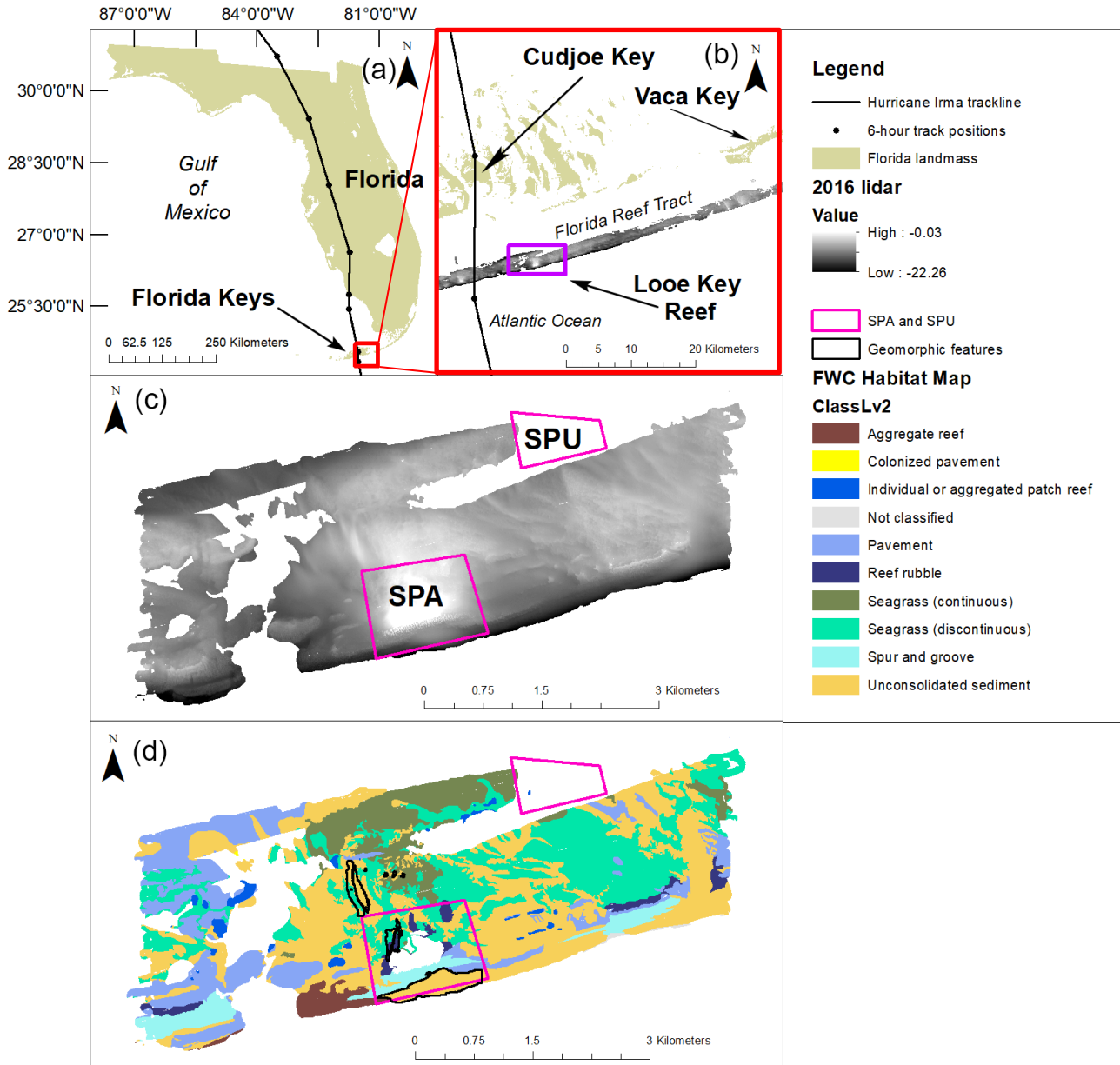
Figure 2. Looe Key Reef location, bathymetry, and seafloor habitats. (a) Location of the Florida Keys along the southern coast of Florida, trackline of Hurricane Irma and the location of its landfall (red box). (b) Proximity of Hurricane Irma's trackline to the Looe Key Reef study site (purple box), location of landfall at Cudjoe Key, and location of Vaca Key where the nearest NOAA-NOS (2023) Tides and Currents station was located. (c) 2016 lidar bathymetric map of the Looe Key Reef study site showing location of Florida Keys National Marine Sanctuary Special Preservation Area (SPA), Special Use Area (SPU), and geomorphic features of focused investigation for this study. (d) Habitat distribution at the Looe Key Study site from Florida Fish and Wildlife Conservation Commission-Fish and Wildlife Research Institute (2015).

km away from the storm's center, and hurricane force winds more than 125 km from the storm's center (NWS, 2022b). Gale force winds (sustained winds above 63 km h^{-1}) were detected by the evening of 9 September 2017 at the National Oceanic and Atmospheric Administration - National Ocean Service (NOAA-NOS), Tides and Currents Station at Vaca Key (number 8723970), 35 km to the northeast of LKR; maximum sustained winds of 213 km h^{-1} were reported as the storm made landfall, and latent gale force winds were detected after the storm passed on the evening of 10 September 2017 (NOAA-NOS, 2023). The average wind direction for this period was 67.01 degrees indicating winds moved from ENE toward WSW. Wind speeds fell sharply below gale force after the storm, shifting north eastward. Wind conditions were relatively quiescent from July 2016 through January 2019 (except during Hurricane Irma) with wind speeds occasionally ranging up to approximately 56 km h^{-1} during winter storms (NOAA-NOS, 2023).

2.2 Elevation and Habitat Data

Three Digital Elevation Models (DEMs) derived from lidar or multibeam bathymetric surveys were used for seafloor elevation- and volume-change analyses and are referenced in this study as 2016 lidar, 2017 multibeam, and 2019 lidar (Table 1).

Table 1: Elevation datasets used in this analysis; collection dates are specific to the geographic extent of this study.

Digital Elevation Model	Source	Collection Dates	Horizontal Resolution/ Vertical RMSE (meters/meters)
2016 NOAA NGS Topobathy Lidar DEM:Florida Keys Outer Reef Block 01	Office for Coastal Management, 2017	23 July 2016	1.0/0.15
Multibeam bathymetry data collected in December 2017, February and March 2018 at Looe Key, the Florida Keys	Fredericks et al, 2019	Leg 1: 12 December 2017 – 16 December 2017 Leg 2: 2 February 2018 – 9 February 2018 Leg 3: 9 March 2018 –11 March 2018	1.0/0.14
2018-2019 NOAA NGS Topobathy Lidar Hurricane Irma: Miami to Marquesas Keys, FL	National Geodetic Survey, 2022	8 January 2019– 31 January 2019	1.0/0.11

RMSE = root mean square error.

The 2016 lidar DEM refers to data that were collected on 23 July 2016 (13.5 months before the passage of Hurricane Irma) by the NOAA Office for Coastal Management, National Geodetic Survey, Topobathy Lidar Dem Block 1 dataset (Office for Coastal Management, 2017). The 2017 multibeam DEM refers to multibeam bathymetry data collected by the U.S. Geological

Survey in December 2017, and February–March 2018 at Looe Key Reef (between three and six months after the passage of Hurricane Irma), specifically to examine impacts from the storm (Fredericks et al., 2019). The 2019 lidar DEM refers to data collected January 8–31, 2019 by NOAA NGS Topobathy Lidar DEM Hurricane Irma: Miami to Marquesas Keys, FL dataset

175 (National Geodetic Survey, 2022). The Florida Fish and Wildlife Conservation Commission (FWC) Unified Florida Reef Tract (UFRT) Map version 2.0, Level 2 habitat categories (FWC, 2015) were used to delineate geographic boundaries for 10 habitat types within the LKR study site (Fig. 2d). Habitat labelled as 'not classified' was indistinguishable during mapping due to turbidity, cloud cover, water depth, or other interferences with obtaining an optical signature of the seafloor (Zitello et al., 2009).

180 **2.3 Elevation- and Volume-Change Analyses**

Seafloor elevation- and volume-change analyses were conducted using the methods of Yates et al. (2017) and 2-m grid spacing techniques of Murphy et al. (2022) (Fig. 3a). Briefly, individual geographic footprint areas (polygons) were created for each of the three 1-m resolution digital elevation models (DEMs) in ArcMap 10.7 and were used to create a common footprint polygon shapefile for the total LKR study site encompassing the overlapping area among the three datasets. The original (full

185 areal extent, or unclipped) 2016–2017 elevation-change data set was 19.71 km^2 and included 4,934,364 data points. The overlapping areal extent for the 2016, 2017, and 2019 DEMs was 15.98 km^2 and excluded areas where water depths were too shallow for boat access to collect multibeam data in 2017 and areas of coarse interpolation within the 2017 DEM. The areal extent of each DEM was then clipped to the areal extent of the common overlapping footprint prior to elevation change analysis using the 'Clip' tool in ArcMap. The following steps were performed in Global Mapper 22.1 due to file size limitations in

190 ArcMap. A 2-m XY grid was created in Global Mapper and clipped to the same footprint. Elevation values were then extracted from each of the three DEMs at the center points of co-aligned 2-m grid boxes. Elevation change between time periods was calculated for each of 4,007,961 paired elevation values (e.g., 2017 elevation – 2016 elevation, and 2019 elevation – 2017 elevation). Elevation-change (XYZ) point maps were generated as shapefiles for each time-period of change for the total study site; positive values indicate an increase in elevation and negative values indicate a decrease in elevation. We used these

195 changes in elevation to estimate the net effect of all processes affecting accretion and erosion in the system; and use of these terms for our study indicates estimates of net accretion and net erosion from our measurements. Data are available from Fehr et al. (2021). Vertical uncertainty of elevation change analyses was estimated using methods of Yates et al. 2017 and the reported vertical accuracy of the lidar and multibeam data sets (typically reported as the 95% root-mean-square error, RMSE, Table 1) to calculate a composite RMSE (RMSE$_{Total}$) for each elevation change analysis (Fig. 3b). The RMSE of lidar and

200 multibeam data sets used for elevation-change analyses in our study ranged from 0.11 to 0.15 m (Table 1). These values are consistent with RMSEs determined in performance evaluations of lidar sensors that ranged from 0.08 to 0.52 m (Fernandez-Diaz et al., 2014; Legleiter et al., 2016; Kinzel et al., 2013; Tonina et al., 2019; Yoshida et al., 2022). Composite RMSE values for elevation-change analyses based on comparison of lidar to multibeam DEMs ranged from 0.19 to 0.21m in our study. These values are consistent with RMSEs determined in performance evaluations of lidar sensors against multibeam echosounders

205 that ranged from 0.02 to 0.23 m (Awadallah et al., 2023). The FWC UFRT habitat map was clipped to the intersect footprint for each elevation-change analysis using ArcMap 10.7. Each total-study-site elevation-change data set was then clipped to individual habitat polygons to create individual elevation-change shapefiles for each habitat type.

Elevation-change data from each time-period were then used to generate TIN (Triangulated Irregular Network) surface models
210 in ArcMap for calculation of volume change. TIN models were clipped to the original overall study site intersect footprint to remove interpolation across areas where no data were collected. Lower bound (conservative) volume-change was calculated
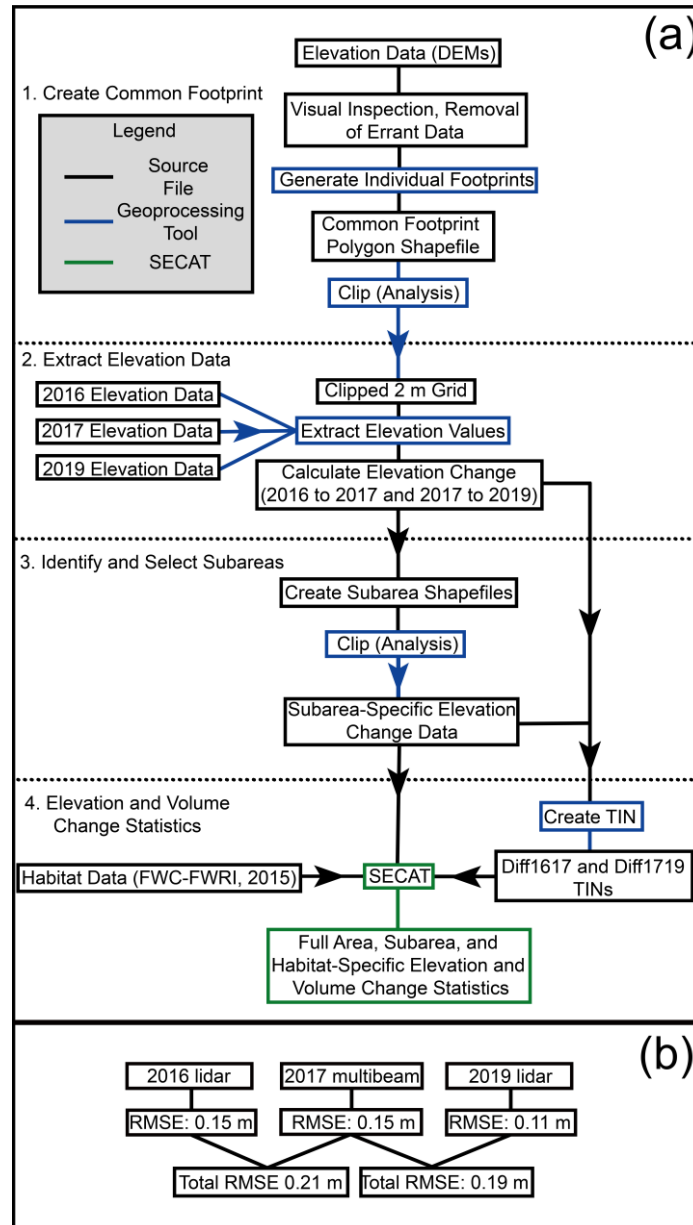
$$RMSE_{total} = \sqrt{(RMSE^2_{Source\ Dataset\ 1} + RMSE^2_{Source\ Dataset\ 2})}$$

Figure 3. Seafloor elevation and volume change methods. (a) Flowchart outlining generalized geoprocessing steps in ArcMap and Global
215 Mapper (steps 1 through 3), and in the Seafloor Elevation Change Analysis Tool (SECAT, step 4) for seafloor elevation and volume change
analyses based on Yates et al. (2017), Murphy et al. (2022), and Zieg and Zawada (2021). (b) Composite RMSE ($RMSE_{Total}$) for each
elevation change analysis (2016 to 2017 and 2017 to 2019) calculated using reported RMSE for lidar and multibeam source data and methods
of Yates et al. (2017). Black boxes indicate source data files. Blue boxes indicate steps using geoprocessing tools from ArcMap or Global
Mapper. Green boxes indicate data analysis conducted using SECAT.

220

based on areal volume above and below surface plane heights corresponding to plus and minus the $RMSE_{Total}$ of the elevation

change analysis ($RMSE_{Total}$ = 21 cm for 2016 to 2017, and 19 cm for 2017 to 2019 change analyses). Upper bound volume

changes were calculated based on area volume above and below a plane height of 0 m. The attribute values stored within the

elevation-change and TIN surface shapefiles were then used to compute elevation and volume change statistics for the total

225 LKR study site and each habitat type using the Seafloor Elevation Change Analysis Tool (SECAT) custom Python script of

Zieg and Zawada (2021). Pearson correlation and linear regression analyses were performed using Microsoft Excel Version

2302 (build 16.0.16130.20690) to assess relationships between mean habitat water depth, elevation change, and area-

normalized volume change for each habitat type including: 1) 2016 mean water depth (estimated from mean elevation) and

mean elevation change; 2) 2016 mean water depth and area-normalized volume change; 3) 2017 mean water depth and mean

230 elevation change; 4) 2017 mean water depth and area-normalized volume change; and 5) 2017 to 2019 mean elevation change

and 2016 to 2017 mean elevation.

2.4 Geomorphic Feature Analyses

Sub-areas or geomorphic features of high-magnitude elevation change (greater than approximately ±0.5 m) were delineated

on each total-study-site elevation-change point map by manually drawing polygons in ArcMap 10.7 and creating elevation-

235 change shapefiles for each sub-area. Each sub-area was clipped to individual habitat polygons to create individual shapefiles

for each habitat type within a given sub-area. Elevation- volume-change statistics were computed for each geomorphic feature

of interest, and each habitat within sub-areas of interest using SECAT and methods described in section 2.3.

We examined elevation and elevation-change along four 200 to 300 m transects across examples of high-elevation change

240 geomorphic features. Elevation profiles for 2016, 2017, and 2019 were created for each feature of interest by extracting

elevation values from each DEM along transect lines across the areas of greatest elevation change for each feature using

ArcMap. Points were selected using the Select Feature by Line tool in ArcMap, and the selected features were then exported

as a new shapefile. Positions and types of geomorphic features of interest were verified through in-situ observation by SCUBA

divers using methods of Fehr and Yates (2020) at 30 diver reconnaissance sites throughout the total study site.

3 Results

3.1 Elevation and Volume Change Analyses

Elevation-change results for 4,007,961 point-locations at LKR between 2016–2017 (approximately 13.5 months before and 3 to 6 months after Hurricane Irma) and between 2017–2019 (from approximately 3 to 16.5 months after Hurricane Irma) are shown in Fig. 4a and b, respectively. Mean elevation-change for the total LKR study site from 2016–2017 was 0.34 m ± 0.21; and all ten habitat types (Fig. 4c) showed increases in mean elevation (accretion) ranging from 0.20 m to 0.54 m (Table 2). Largest mean elevation changes were associated with 'aggregate reef' (mean 2016 elevation -13.41 m) and 'not classified'
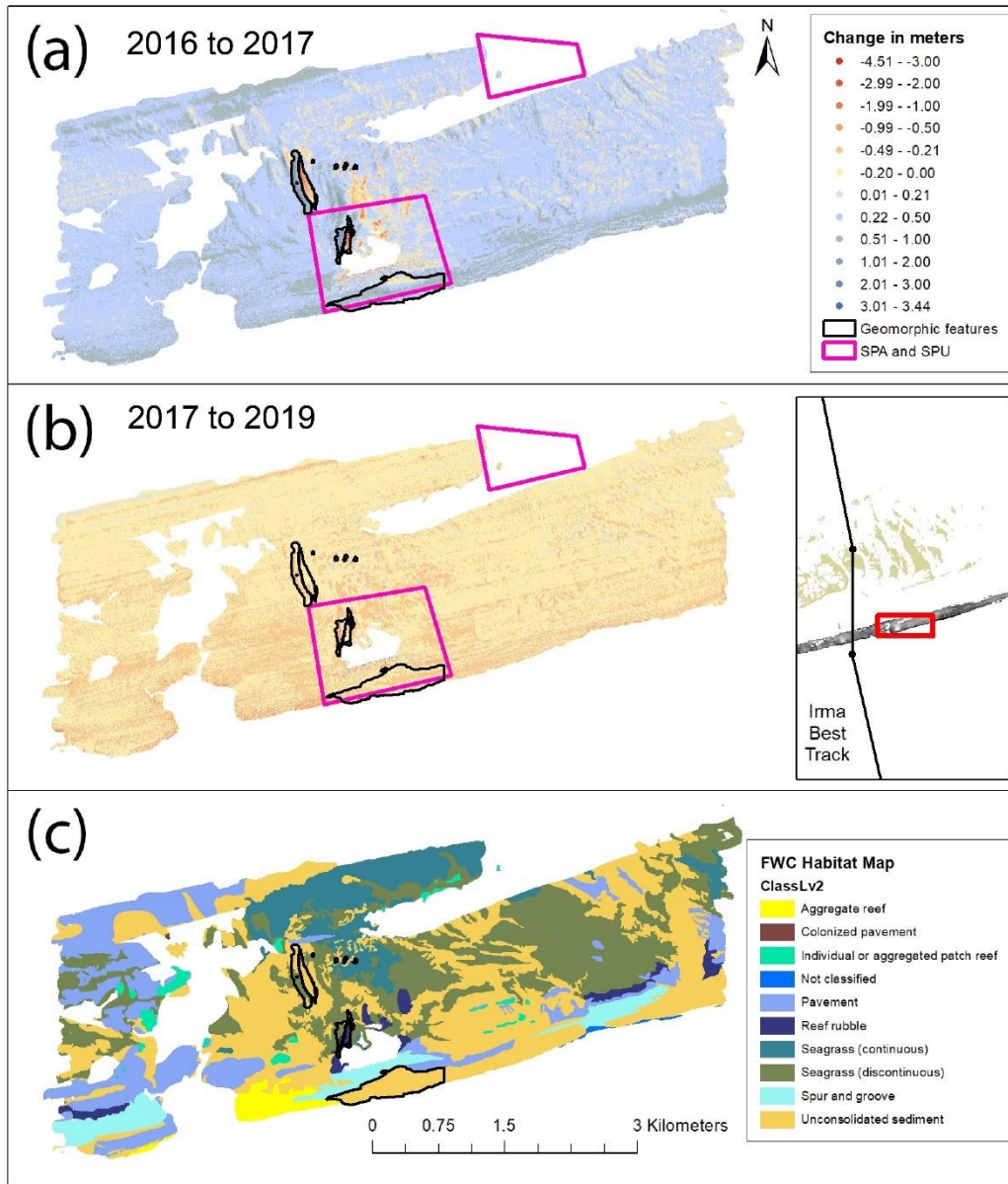
Figure 4. Elevation-change results for 4,007,961 point-locations at Looe Key Reef. Elevation change between (a) 2016 to 2017 (13.5 months before and 3 to 6 months after Hurricane Irma) and (b) between 2017 to 2019 (from approximately 3 to 16.5 months after Hurricane Irma), and (c) corresponding seafloor habitats (FWC, 2015). The Hurricane Irma best track data in the panel b's inset is from the NOAA NHC Irma Storm Track resource page (NHC, 2018, see also Figure 2b). Boundaries for the Looe Key Sanctuary Protection Area (SPA) and Special Protection Unit (SPU) are shown as pink polygons. Geomorphic features of interest are indicated with black polygons. Gaps in map areas indicate locations where water depth was too shallow for collection of multibeam bathymetric data.

260

Table 2. Elevation change data by habitat type associated with each period and geomorphic feature subarea.

Habitat type	Total points (no.)	Area (km²)	Mean elevation (m) 2016	2017	2019	Mean elevation change (m) (SD) 2016 to 2017	2017 to 2019
Overall Looe Key Study Site							
Total Study Site	4007961	15.98	-8.87	-8.53	-8.69	0.34 (0.21)	-0.15 (0.11)
Aggregate Reef	76647	0.30	-13.41	-12.91	-13.16	0.51 (0.20)	-0.25 (0.20)
Colonized Pavement	750	0.0028	-10.65	-10.33	-10.44	0.32 (0.12)	-0.11 (0.08)
Individual or Aggregate Patch Reef	54414	0.22	-8.66	-8.33	-8.51	0.34 (0.15)	-0.19 (0.10)
Not Classified	6932	0.026	-15.84	-15.30	-15.55	0.54 (0.25)	-0.25 (0.17)
Pavement	645001	2.57	-10.00	-9.62	-9.79	0.37 (0.16)	-0.16 (0.11)
Reef Rubble	80987	0.32	-6.19	-5.99	-6.17	0.20 (0.36)	-0.18 (0.12)
Seagrass Continuous	402458	1.60	-7.69	-7.42	-7.54	0.27 (0.18)	-0.12 (0.09)
Seagrass Discontinuous	1067504	4.26	-7.24	-6.96	-7.10	0.28 (0.21)	-0.14 (0.10)
Spur and Groove	184875	0.74	-9.82	-9.45	-9.65	0.37 (0.25)	-0.19 (0.19)
Unconsolidated Sediment	1488416	5.94	-9.63	-9.26	-9.42	0.37 (0.21)	-0.16 (0.09)
Sand Wave							
Total Accretion Area	15336	0.060	-6.32	-5.53	-5.68	0.79 (0.45)	-0.15 (0.12)
Seagrass Discontinuous	7345	0.029	-5.98	-5.08	-5.23	0.90 (0.49)	-0.15 (0.13)
Unconsolidated Sediment	7991	0.031	-6.63	-5.95	-6.09	0.68 (0.37)	-0.14 (0.10)
Total Erosion Area	11265	0.043	-5.40	-5.75	-5.90	-0.36 (0.28)	-0.15 (0.06)
Seagrass Discontinuous	580	0.002	-5.72	-5.87	-6.02	-0.15 (0.15)	-0.15 (0.08)
Unconsolidated Sediment	10685	0.041	-5.38	-5.74	-5.90	-0.37 (0.29)	-0.15 (0.05)
Scour Marks							
Scour Mark 1	202	0.00071	-7.03	-7.51	-7.41	-0.49 (0.26)	0.10 (0.12)
Seagrass Discontinuous	197	0.00071	-7.02	-7.51	-7.41	-0.49 (0.26)	0.11 (0.12)
Unconsolidated Sediment	5	<0.00001	-7.34	-7.47	-7.52	-0.12 (0.03)	-0.05 (0.02)
Scour Mark 2	388	0.0014	-5.41	-5.91	-5.71	-0.50 (0.27)	0.20 (0.20)
Seagrass Continuous	338	0.00124	-5.41	-5.94	-5.70	-0.53 (0.27)	0.24 (0.18)
Unconsolidated Sediment	50	0.00016	-5.42	-5.67	-5.72	-0.26 (0.16)	-0.05 (0.13)
Scour Mark 3	518	0.00188	-5.64	-6.14	-6.02	-0.50 (0.29)	0.12 (0.19)
Seagrass Continuous	518	0.00188	-5.64	-6.14	-6.02	-0.50 (0.29)	0.12 (0.19)
Scour Mark 4	417	0.00152	-5.20	-5.74	-5.63	-0.54 (0.28)	0.12 (0.21)
Seagrass Continuous	411	0.00151	-5.19	-5.74	-5.62	-0.55 (0.27)	0.12 (0.21)
Unconsolidated Sediment	6	0.00001	-5.69	-5.74	-5.84	-0.06 (0.05)	-0.10 (0.05)
Reef Rubble Field							
Total Accretion Area	7216	0.028	-4.22	-3.32	-3.57	0.89 (0.45)	-0.24 (0.30)
Reef Rubble	3102	0.012	-3.71	-2.84	-3.05	0.87 (0.44)	-0.21 (0.36)
Seagrass Discontinuous	3489	0.014	-4.66	-3.67	-3.97	0.99 (0.42)	-0.30 (0.24)
Unconsolidated Sediment	628	0.00237	-4.25	-3.82	-3.91	0.43 (0.26)	-0.10 (0.12)
Total Erosion Area	6043	0.023	-3.00	-3.64	-3.74	-0.63 (0.48)	-0.10 (0.19)
Reef Rubble	3409	0.013	-2.61	-3.39	-3.44	-0.77 (0.50)	-0.06 (0.20)
Seagrass Discontinuous	1941	0.00708	-3.51	-4.05	-4.22	-0.54 (0.43)	-0.17 (0.15)
Unconsolidated Sediment	694	0.00248	-3.50	-3.70	-3.82	-0.20 (0.15)	-0.12 (0.13)
Sand Lobe							
Total Area	67389	0.266	-12.41	-11.90	-12.10	0.51 (0.29)	-0.20 (0.09)
Unconsolidated Sediment	67389	0.266	-12.41	-11.90	-12.10	0.51 (0.29)	-0.20 (0.09)

*58 data points fell on borders between habitats and were counted twice during habitat analysis. SD = standard deviation.

(mean 2016 elevation -15.84 m) habitat types. Smallest mean elevation changes were associated with 'reef rubble' (mean 2016 elevation -6.19 m) and 'seagrass continuous' (mean 2016 elevation -7.69 m) habitats (Table 2). Only 4% of all data points showed losses in elevation (erosion) ranging from -0.01 m to -0.44 m, while 96% of all data points showed gains in elevation ranging from 0.31 m to 0.55 m across all habitats. Pearson correlation analysis showed a very strong positive correlation ($r(8)$ = 0.96, $p = 0.000$) and linear relationship ($r^2 = 0.92$, Fig. 5a) between 2016 mean habitat water depth (estimated from mean elevation) and mean elevation change; mean elevation gains increased significantly with increasing water depth (i.e., decreasing seafloor elevation). Net volume change was up to 5.36 Mm³ over the total 15.98 km² Looe Key study site; and all

habitat types showed increases in net volume (accretion) with upper bound ranges from 0.001 to 2.19 Mm^3 (Table 3). Largest net volume changes were associated with habitats covering the largest areal extent of the study area including 'pavement,' 'discontinuous seagrass,' and 'unconsolidated sediment.' Pearson correlation analysis also indicated a very strong positive correlation ($r(8) = 0.99$, $p = 0.000$) and linear relationship ($r^2 = 0.92$, Fig. 5b) between 2016 mean habitat water depth and area-normalized volume change; area-normalized volume gains increased significantly with increasing water depth. Largest area-normalized volume changes of 0.51 Mm^3 and 0.54 Mm^3 were observed for 'aggregate reef' and 'not classified' habitats, respectively; and smallest changes of 0.20 to 0.27 Mm^3 were observed for 'reef rubble' and 'continuous seagrass' habitats (Table 3), consistent with mean elevation changes for those habitats. Mean elevation-change values of the 2016–2017 elevation change data set that was clipped to an area of 15.98 km^2 and used for this analysis were within ±0.01 m, and area-normalized volumes were within ±0.016 $Mm^3 km^{-2}$, of values calculated in the original 19.71 km^2 published data set (unclipped) for the overall study site and all habitats (Yates et al., 2019).

Mean elevation-change during a 13-month time-period between December 2017 to June 2019 (up to approximately 16.5 months after Hurricane Irma) was $-0.15 ± 0.11$ m, and all habitat types showed losses in mean elevation ranging from -0.11 m to -0.25 m (Fig. 4b, Table 2). Largest mean elevation changes were associated with 'aggregate reef' and 'not classified' habitat types, and smallest changes were associated with 'colonized pavement' and 'continuous seagrass' habitats (Table 2). Only 5% of all data points showed gains in elevation with mean accretion ranging from 0.04 m to 0.19 m, while 95% of all data points showed losses in elevation with mean erosion ranging from -0.13 m to -0.27 m across all habitat types. Pearson correlation analysis indicated a moderate correlation ($r(8) = -0.67$, $p = 0.035$) and linear relationship ($r^2 = 0.45$, Fig. 5c) between estimated 2017 mean habitat water depth and mean elevation change; mean elevation loss generally increased with increasing water depth. Net volume change was up to -2.46 Mm^3 over the total 15.98 km^2 Looe Key study site and area-normalized volume change was -0.15 $Mm^3 km^{-2}$. Losses in net volume up to -0.931 Mm^3 (erosion) were observed across all habitat types (Table 4).

Largest net volume changes were associated with habitats covering the largest areal extent of the study area including 'pavement,' 'discontinuous seagrass,' and 'unconsolidated sediment.' Pearson correlation analysis indicated a moderate correlation ($r(8) = -0.67$, $p = 0.035$) and linear relationship ($r^2 = 0.45$, Fig. 5d) between 2017 mean habitat water depth and area-normalized volume change; area-normalized volume losses generally increased with increasing water depth. Largest area-normalized volume changes were observed for 'aggregate reef' and 'not classified' habitats, -0.254 and -0.247 $Mm^3 km^{-2}$, respectively; smallest changes were observed for 'colonized pavement' and 'continuous seagrass' habitats, -0.112 to -0.118 $Mm^3 km^{-2}$ respectively (Table 4), consistent with mean elevation changes for those habitats. Pearson correlation analysis indicated a strong negative correlation ($r(8) = -0.74$, $p = 0.014$) and linear relationship ($r^2 = 0.55$, Fig. 5e) between 2017 to 2019 mean habitat elevation change and 2016 to 2017 mean habitat elevation change; mean elevation losses during 2017 to 2019 were significantly greater in habitats with larger mean elevation gains during 2016 to 2017. Mean elevation change (loss)

305   during 2017 to 2019 was 35 to 55% of the mean elevation change (gain) during 2016 to 2017 for all habitats except for reef rubble which was 92% and had the shallowest mean depth (6.0 m) of all habitats.
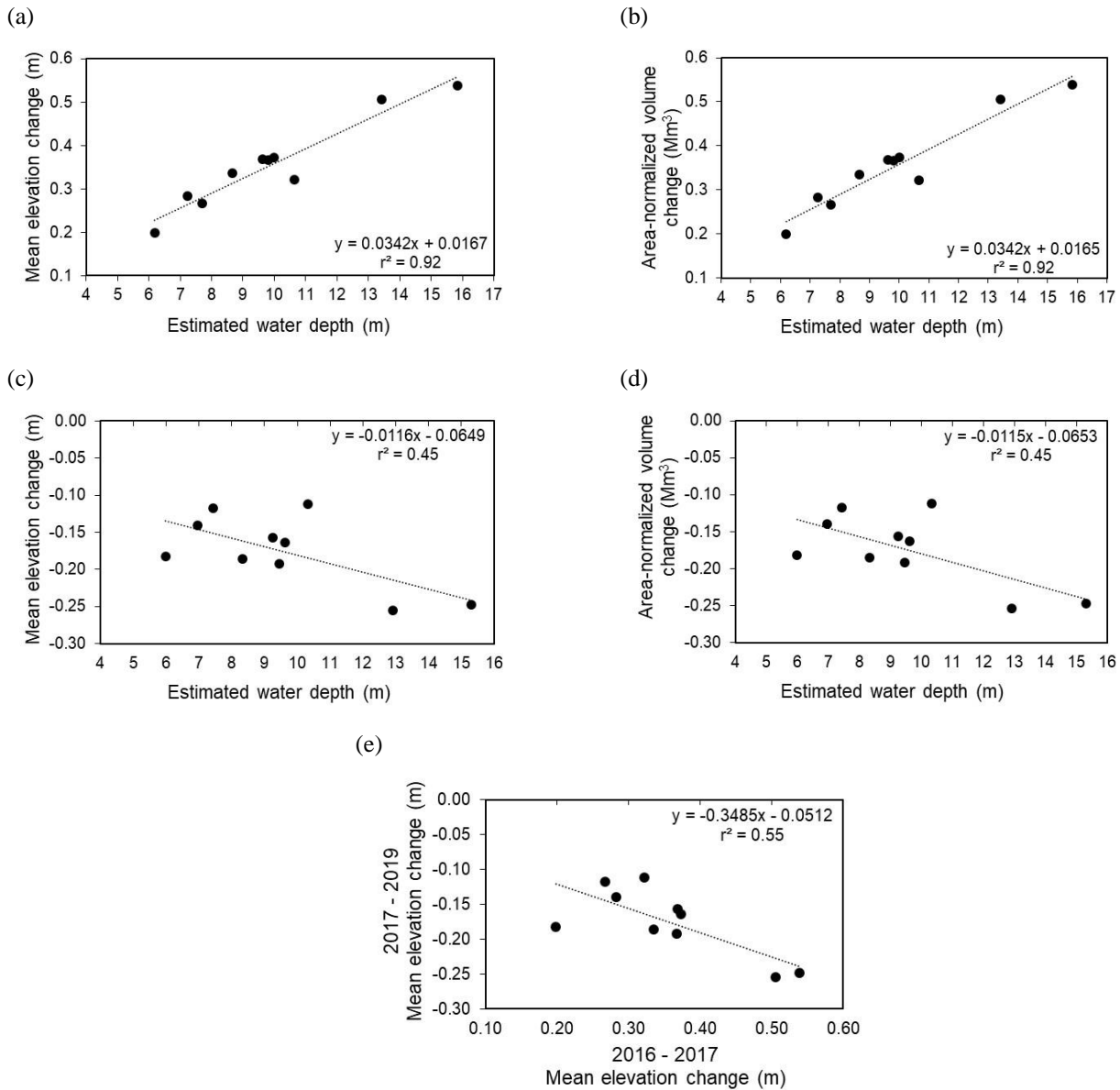
Figure 5. Linear relationships between elevation change, volume change, and water depth. Linear relationships and coefficients of determination between (a) mean elevation change, (b) mean area-normalized volume change, and estimated 2016 mean water depth for

310   seafloor habitats of the Looe Key study site between 2016 to 2017. Linear relationships and coefficients of determination between (c) mean elevation change, (d) mean area-normalized volume change, and estimated 2017 mean water depth for seafloor habitats of the Looe Key study site between 2017 to 2019 (a, b). Linear relationship between 2017 to 2019 mean elevation change and 2016 to 2017 mean elevation change (e).

315   **Table 3. Compiled volume change data by habitat type for all study areas during the 2016 to 2017 study period (storm period).**

Habitat Type	Habitat Area (km²)	Gross erosion (Mm³)		Gross accretion (Mm³)		Net volume change (Mm³ study-area⁻¹)		Area-normalized volume change (Mm³ km⁻²)	
		Lower	Upper	Lower	Upper	Lower	Upper	Lower	Upper
Overall Looe Key Study Site									
Total Study Site	15.98	0.053	0.134	2.456	5.490	2.403	5.356	0.150	0.335
Aggregate Reef	0.30	0	0	0.090	0.154	0.090	0.154	0.296	0.505
Colonized Pavement	0.0028	0	0	0	0.001	0	0.001	0.124	0.323
Individual or Aggregate Patch Reef	0.22	0	0	0.029	0.073	0.029	0.072	0.136	0.336
Not Classified	0.026	0	0	0.009	0.014	0.009	0.014	0.337	0.540
Pavement	2.57	0	0.003	0.445	0.962	0.445	0.959	0.173	0.373
Reef Rubble	0.32	0.013	0.021	0.033	0.085	0.020	0.064	0.062	0.199
Seagrass Continuous	1.60	0.008	0.021	0.152	0.449	0.144	0.428	0.090	0.267
Seagrass Discontinuous	4.26	0.015	0.045	0.477	1.250	0.462	1.205	0.109	0.283
Spur and Groove	0.74	0.003	0.007	0.136	0.278	0.133	0.271	0.181	0.367
Unconsolidated Sediment	5.94	0.013	0.037	1.083	2.226	1.070	2.189	0.180	0.369
Sand Wave									
Total Accretion Area	0.060	0	0	0.036	0.048	0.036	0.048	0.598	0.800
Seagrass Discontinuous	0.029	0	0	0.020	0.026	0.020	0.026	0.709	0.914
Unconsolidated Sediment	0.031	0	0	0.015	0.021	0.015	0.021	0.494	0.694
Total Erosion Area	0.043	0.009	0.016	0	0	-0.009	-0.016	-0.198	-0.370
Seagrass Discontinuous	0.002	<0.001	<0.001	0	0	<-0.001	<-0.001	-0.045	-0.162
Unconsolidated Sediment	0.041	0.008	0.016	0	0	-0.008	-0.016	-0.205	-0.380
Scour Marks									
Scour Mark 1	0.00071	0.0002	0.0004	0	0	-0.0002	-0.0004	-0.3083	-0.5114
Seagrass Discontinuous	0.00071	0.0002	0.0004	0	0	-0.0002	-0.0004	-0.3118	-0.5154
Unconsolidated Sediment	<0.00001	0	0	0	0	0	<-0.0001	-0.0001	-0.1479
Scour Mark 2	0.0014	0.0005	0.0007	0	0	-0.0005	-0.0007	-0.3255	-0.5271
Seagrass Continuous	0.00124	0.0004	0.0007	0	0	-0.0004	-0.0007	-0.3558	-0.5595
Unconsolidated Sediment	0.00016	0	<-0.0001	0	0	0	<-0.0001	-0.0943	-0.2790
Scour Mark 3	0.00188	0.0006	0.0010	0	0	-0.0006	-0.0010	-0.3247	-0.5232
Seagrass Continuous	0.00188	0.0006	0.0010	0	0	-0.0006	-0.0010	-0.3247	-0.5232
Scour Mark 4	0.00152	0.0006	0.0009	0	0	-0.0006	-0.0009	-0.3631	-0.5661
Seagrass Continuous	0.00151	0.0006	0.0009	0	0	-0.0006	-0.0009	-0.3658	-0.5697
Unconsolidated Sediment	0.00001	0	<-0.0001	0	0	0	<-0.0001	0.0000	-0.0748
Reef Rubble Field									
Total Accretion Area	0.028	0	0	0.020	0.025	0.020	0.025	0.707	0.914
Reef Rubble	0.012	0	0	0.008	0.011	0.008	0.011	0.690	0.897
Seagrass Discontinuous	0.014	0	0	0.011	0.014	0.011	0.014	0.802	1.011
Unconsolidated Sediment	0.002	0	0	0.001	0.001	0.001	0.001	0.252	0.446
Total Erosion Area	0.023	0.011	0.015	0	0	-0.011	-0.015	-0.464	-0.661
Reef Rubble	0.013	0.008	0.010	0	0	-0.008	-0.010	-0.584	-0.788
Seagrass Discontinuous	0.007	0.003	0.004	0	0	-0.003	-0.004	-0.382	-0.577
Unconsolidated Sediment	0.002	0.000	0.001	0	0	0.000	-0.001	-0.064	-0.221
Sand Lobe									
Total Area	0.27	0	0.002	0.089	0.139	0.089	0.137	0.332	0.513
Unconsolidated Sediment	0.27	0	0.002	0.089	0.139	0.089	0.137	0.332	0.513

'Upper' and 'lower' headings refer to the upper and lower bounds of volume change based on total RMSE root mean square error). Lower bounds use total RMSE as a plane height in calculating volume.

320

Table 4. Compiled volume change data by habitat type for all study areas during the 2017 to 2019 study period (post-storm re-equilibration period).

Habitat Type	Habitat Area (km^2)	Gross erosion (Mm^3)		Gross accretion (Mm^3)		Net volume change (Mm^3 study-area^{-1})		Area-normalized volume change (Mm^3 km^{-2})	
		Lower	Upper	Lower	Upper	Lower	Upper	Lower	Upper
Overall Looe Key Study Site									
Total Study Site	15.98	0.316	2.502	0.005	0.041	-0.311	-2.461	-0.019	-0.154
Aggregate Reef	0.30	0.028	0.078	0	<0.001	-0.028	-0.077	-0.093	-0.254
Colonized Pavement	0.0028	<0.001	<0.001	0	0	<-0.001	<-0.001	-0.004	-0.112
Individual or Aggregate Patch Reef	0.22	0.006	0.040	0	0	-0.006	-0.040	-0.028	-0.186
Not Classified	0.026	0.002	0.007	0	<0.001	-0.002	-0.006	-0.083	-0.247
Pavement	2.57	0.059	0.424	0	0.004	-0.059	-0.420	-0.023	-0.163
Reef Rubble	0.32	0.010	0.061	0.001	0.002	-0.009	-0.059	-0.029	-0.182
Seagrass Continuous	1.60	0.012	0.197	0.001	0.008	-0.011	-0.189	-0.007	-0.118
Seagrass Discontinuous	4.26	0.064	0.612	0.001	0.015	-0.063	-0.597	-0.015	-0.140
Spur and Groove	0.74	0.032	0.145	0.001	0.003	-0.031	-0.141	-0.042	-0.192
Unconsolidated Sediment	5.94	0.102	0.938	0.000	0.007	-0.102	-0.931	-0.017	-0.157
Sand Wave									
Total Accretion Area	0.060	0.0015	0.0093	0	0.0005	-0.0015	-0.0088	-0.0245	-0.1479
Seagrass Discontinuous	0.029	0.0010	0.0048	0	0.0003	-0.0010	-0.0044	-0.0336	-0.1544
Unconsolidated Sediment	0.031	0.0005	0.0045	0	0.0001	-0.0005	-0.0044	-0.0159	-0.1419
Total Erosion Area	0.043	0.0003	0.0066	0	0	-0.0003	-0.0066	-0.0074	-0.1529
Seagrass Discontinuous	0.002	<0.0001	0.0003	0	0	<-0.0001	-0.0003	-0.0158	-0.1521
Unconsolidated Sediment	0.041	0.0003	0.0063	0	0	-0.0003	-0.0063	-0.0070	-0.1529
Scour Marks									
Scour Mark 1	0.00071	0.0000	0.0000	<0.0001	0.0001	<0.0001	0.0001	0.0171	0.1201
Seagrass Discontinuous	0.00071	0.0000	0.0000	<0.0001	0.0001	<0.0001	0.0001	0.0173	0.1219
Unconsolidated Sediment	<0.00001	0.0000	<0.0001	0.0000	0.0000	0.0000	<-0.0001	0.0000	-0.0447
Scour Mark 2	0.0014	0	0	0.0001	0.0003	0.0001	0.0003	0.0880	0.2226
Seagrass Continuous	0.00124	0	0	0.0001	0.0003	0.0001	0.0003	0.0996	0.2550
Unconsolidated Sediment	0.00016	<0.0001	<0.0001	0	0	<-0.0001	<-0.0001	-0.0009	-0.0254
Scour Mark 3	0.00188	0	0	0.0001	0.0003	0.0001	0.0003	0.0524	0.1380
Seagrass Continuous	0.00188	0	0	0.0001	0.0003	0.0001	0.0003	0.0524	0.1380
Scour Mark 4	0.00152	0	0	0.0001	0.0002	0.0001	0.0002	0.0615	0.1334
Seagrass Continuous	0.00151	0	0	0.0001	0.0002	0.0001	0.0002	0.0620	0.1351
Unconsolidated Sediment	0.00001	0.0000	<0.0001	0.0000	0.0000	0.0000	<-0.0001	0.0000	-0.1029
Reef Rubble Field									
Total Accretion Area	0.028	0.0040	0.0080	0.0010	0.0010	-0.0040	-0.0070	-0.1310	-0.2480
Reef Rubble	0.012	0.0020	0.0040	0	0.0010	-0.0010	-0.0030	-0.1260	-0.2180
Seagrass Discontinuous	0.014	0.0020	0.0040	0	0	-0.0020	-0.0040	-0.1560	-0.3020
Unconsolidated Sediment	0.002	<0.0001	<0.0001	0	0	<-0.0001	<-0.0001	-0.0070	-0.0910
Total Erosion Area	0.023	0.0005	0.0031	0.0003	0.0008	-0.0002	-0.0023	-0.0084	-0.1026
Reef Rubble	0.013	0.0001	0.0015	0.0003	0.0007	0.0002	-0.0008	0.0113	-0.0612
Seagrass Discontinuous	0.007	0.0003	0.0013	0	0.0001	-0.0003	-0.0012	-0.0429	-0.1741
Unconsolidated Sediment	0.002	<0.0001	0.0003	0	0	<-0.0001	-0.0003	-0.0152	-0.1188
Sand Lobe									
Total Area	0.27	0.010	0.055	0	<0.001	-0.010	-0.054	-0.038	-0.204
Unconsolidated Sediment	0.27	0.010	0.055	0	<0.001	-0.010	-0.054	-0.038	-0.204

'Upper' and 'lower' headings refer to the upper and lower bounds of volume change based on total RMSE (root mean square error).

3.2 Geomorphic Feature Analyses

Large-scale geomorphic features that were 10s to 100s of m^2 in areal extent and showed extensive erosion and/or accretion with elevation-changes greater than 0.5 m were observed between 2016 and 2017 (Fig. 6 and 7). Examples of these features included migration of a sand wave in the back reef area of Looe Key reef indicated by adjacent areas of erosion and accretion.

Several scour features developed in 'discontinuous seagrass' and 'unconsolidated sediment' habitats of the Looe Key back reef, indicated by areas of erosion that appear as pits. Rubble fields within and near the Looe Key SPA area were displaced, as indicated by adjacent areas of accretion and erosion. Substantial deposition of sediments occurred along a sand lobe at the base of the Looe Key Reef 'spur and groove' habitat.

3.2.1 Sand Wave

Migration of a sand wave was observed in the back reef area of Looe Key Reef between 2016 and 2017, with minor erosion of this feature occurring between 2017 and 2019 (Fig. 6a, b, and c). The sand wave was approximately 733 m long and 104 m wide at its widest point in 2017, 2 m in height from the crest to base on the deepest (western) edge, with average water depth of approximately 5.6 m. Transect elevation profiles showed the location of this feature in 2016, westward migration of approximately 78 m (crest to crest) in 2017, and minor erosion in 2019 (Fig. 7a). An accretion of 0.060 km^2 included approximately 50% discontinuous seagrass and 50% unconsolidated sediment habitat.

Between 2016 and 2017, mean elevation change of the accretion area (2017 location of the sand wave) was 0.79 m (Table 2) with a maximum elevation gain at the crest of 1.84m. An adjacent area of erosion was approximately 630 x 122 m in length and width (0.043 km^2) and included approximately 5% discontinuous seagrass and 95% unconsolidated sediment. Mean elevation-change of the erosion area was -0.36 m (Table 2) with a maximum elevation loss of -1.23 m near the 2016 location of the sand wave crest. Total net volume change for the accretion area of the feature was 0.048 Mm^3 and area-normalized volume change was 0.800 Mm^3 km^{-2} (Table 3). Mean elevation-change and area-normalized volume change was greatest within the discontinuous seagrass habitat (0.90 m and 0.914 Mm^3 km^{-2}, respectively), approximately 2.7 times greater than mean elevation change and area-normalized volume change for the overall Looe Key study site. It accounted for 55% of total net volume gain, indicating burial of seagrass habitat during migration of the sand wave. Net volume change of the erosion area was approximately -0.016 Mm^3 and area-normalized volume change -0.37 Mm^3 km^{-2} with 98% of net volume change associated with erosion of unconsolidated sediment habitat (Table 3).

Between 2017 and 2019, the sand wave (accretion area) showed mean elevation and net volume change of approximately -0.15 m and approximately -0.009 Mm^3, respectively (Table 2, 4 and Fig. 6b). Similar mean elevation change values were observed for discontinuous seagrass and unconsolidated sediment habitats associated with the feature, and net volume change for each habitat was approximately 50% of the total net volume change (Table 4). Area-normalized volume change was similar for the total area of the sand wave and the sub-areas within it, including discontinuous seagrass and unconsolidated sediment habitats, ranging from approximately -0.148 to -0.154 Mm^3/km^2. The adjacent erosion area (original 2016 location of the sand wave) also showed a mean elevation change of -0.15 m with similar values for the associated discontinuous seagrass and unconsolidated sediment habitats. Net volume change of the erosion area was approximately -0.007 Mm^3 with approximately

95% of this loss associated with unconsolidated sediment (Table 4). Area-normalized volume change was also consistent across the total erosion feature area, discontinuous seagrass, and unconsolidated sediment habitats at -0.15 Mm^3 km^{-2}.
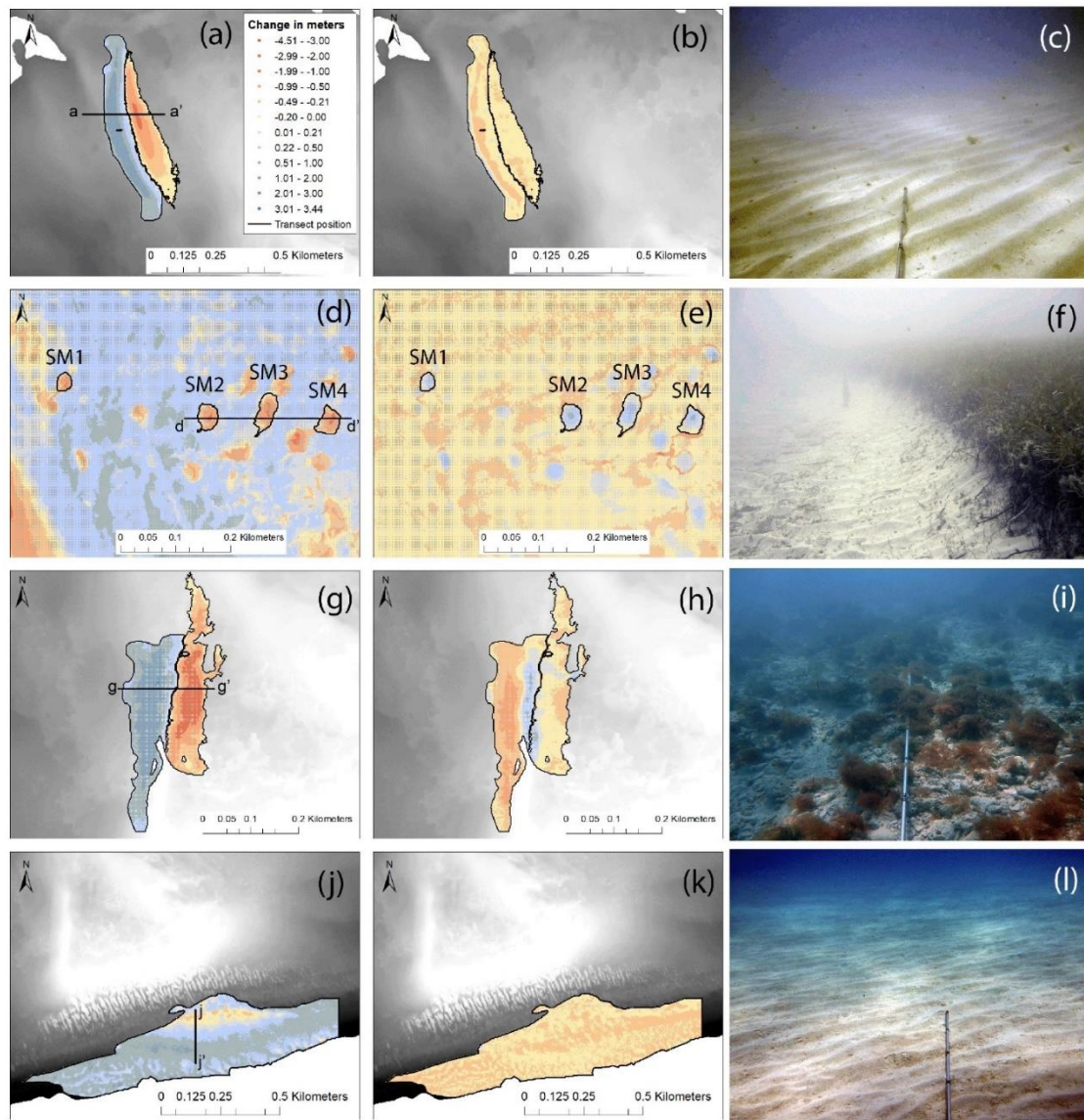
Figure 6. Elevation change data and transect positions for each geomorphic feature subarea. Geomorphic features included a sand wave (a, b, c), scour marks (d, e, f), western rubble field (g, h, i), and sand lobe subareas (j, k, l). These feature locations and corresponding habitat are also shown in Fig. 4. Elevation-change from 2016 to 2017 (a, d, g, j), 2017 to 2019 (b, e, h, k), and corresponding reconnaissance imagery (c, f, i, l) Transect positions are indicated by black lines and lowercase letters in the elevation change panels (see also Fig. 7). Scour marks in panels d and e are labelled SM1 through 4. Photo credit: Mitch Lemon, Cherokee Nations System Solutions for U.S. Geological Survey.
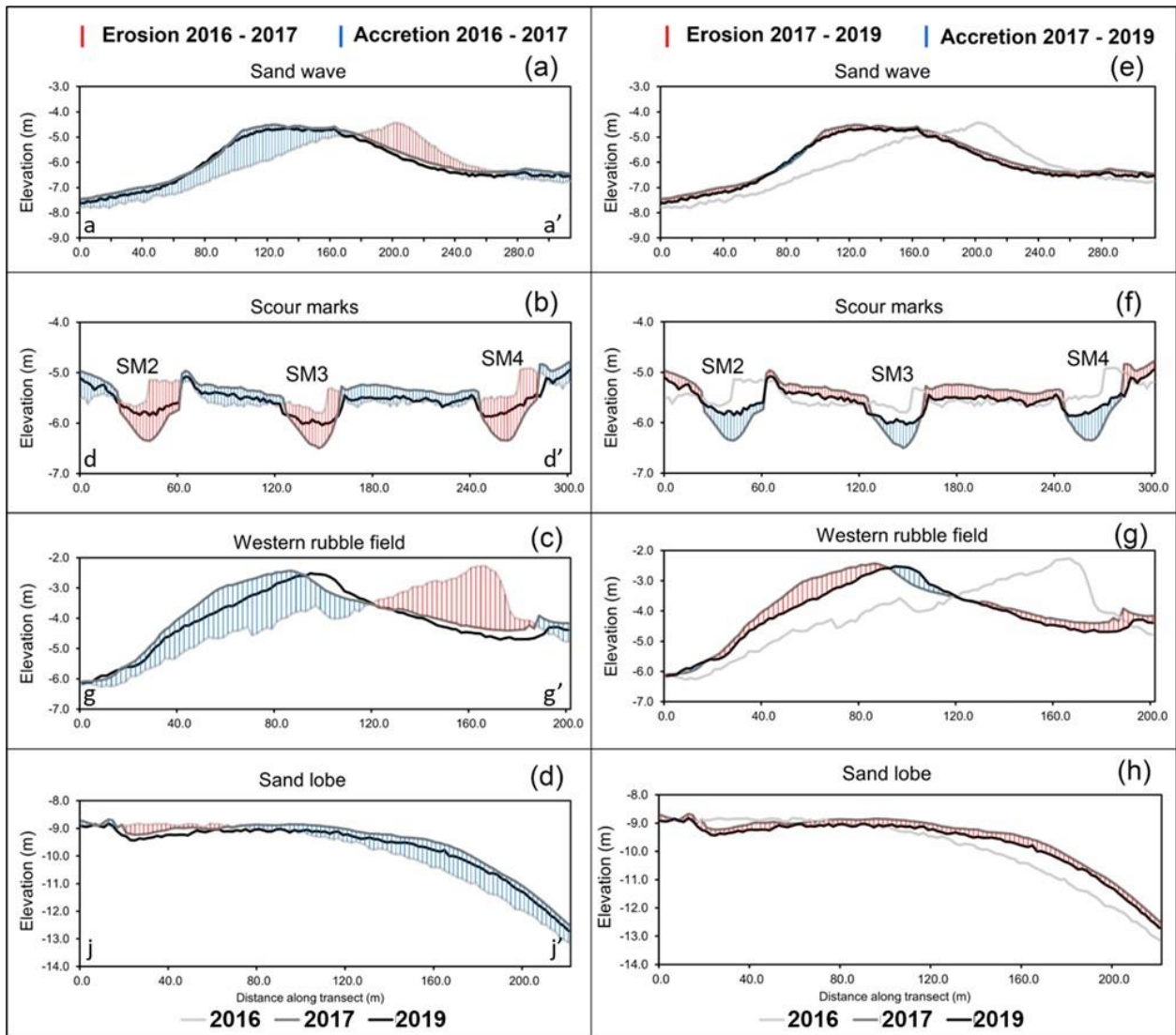
Figure 7. Elevation transects across geomorphic features in 2016, 2017, and 2019. Geomorphic features included a sand wave (a, e), scour marks (b, f), western reef rubble field (c, g), and a sand lobe (d, h). Lowercase letters indicate direction of transects as shown in Figure 6. Vertical red lines indicate areas of erosion and vertical blue lines indicate areas of accretion between (a-d) 2016 and 2017 (before and after Hurricane Irma) and between (e-f) 2017 and 2019. SM = scour mark.

3.2.2 Scour Marks

Development of scour marks was observed in seagrass and unconsolidated sediment habitats in the back reef area of Looe Key Reef between 2016 and 2017 (Fig. 6d, e, and f). These features ranged from approximately 30 to 60 m in length and width with average depths of approximately 5.7 to 7.5 m in 2017. Visual validation of select scour features indicated they developed

between 2016 and 2017 at the edges of seagrass beds where small (approximately 0.5 m) ledges marked the transition between the slightly higher elevation of seagrass beds and lower elevation of adjacent unconsolidated sediment (Fig. 6f). Transect analyses showed considerable erosion of the western boundaries of seagrass beds, development of pit-like features up to approximately 20 m in diameter and 1 m deep, transport of sediment westward, and burial of seagrass between scour features (Fig. 7b). Scour marks showed some infilling between 2017 and 2019. Validation imagery showed exposed rhizomatous growth at the western edges of seagrass beds (Fig. 8).

Elevation- and volume-change analyses were performed on four examples of these features (Fig. 6d and e). Scour mark 1 was 714 m^2 with 99% of the area consisting of discontinuous seagrass. Between 2016 and 2017, mean elevation change was -0.49 m (Table 2) with a maximum observed change of -1.09 m. Net volume change was less than -0.001 Mm^3, and area-normalized volume change was approximately -0.51 Mm^3 km^{-2} (Table 3). Between 2017 and 2019, this feature showed accretion with mean elevation change of 0.10 m and a net volume change of less than 0.001 Mm^3 (Tables 2 and 4). Area-normalized volume change was approximately 0.12 Mm^3 km^{-2}. Scour mark 2 was 1,400 m^2 with 88% of the area consisting of continuous seagrass and 12% unconsolidated sediment. Between 2016 and 2017, mean elevation change was -0.50 m (Table 2) with maximum observed change of -1.28 m. Net volume change was less than -0.001 Mm^3 and area-normalized volume change was approximately -0.53 Mm^3 km^{-2} (Table 3). Ninety-four percent of net volume change was associated with continuous seagrass habitat, which also had the highest area-normalized volume change of -0.56 Mm^3 km^{-2}. Between 2017 and 2019, this feature showed accretion with mean elevation change of 0.20 m and net volume change of 0.0003 Mm^3 (Tables 2 and 4). Continuous seagrass showed an increase in mean elevation (0.24 m) and net volume (0.0003 Mm^3) while unconsolidated sediment showed a decrease in mean elevation (-0.05 m) and net volume (less than -0.0001 Mm^3). Area-normalized volume change across the entire scour mark was approximately 0.22 Mm^3 km^{-2}. Scour mark 3 was 1,882 m^2 with 100% of the area consisting of continuous seagrass. Between 2016 and 2017, mean elevation change was -0.50 m with a maximum observed change of -1.25 m (Table 2). Net volume change was -0.001 Mm^3 and area-normalized volume change was approximately -0.52 Mm^3 km^{-2} (Table 3). Between 2017 to 2019, this feature showed accretion with mean elevation change of 0.12 m and net volume change of 0.0003 Mm^3 (Tables 2 and 4). Area-normalized volume change was approximately 0.14 Mm^3 km^{-2}. Scour mark 4 was 1,520 m^2 with 99% of area consisting of continuous seagrass and 1% unconsolidated sediment. Between 2016 and 2017, mean elevation change was -0.54 m with a maximum observed change of -1.29 m (Table 2). Net volume change was -0.0009 Mm^3 and area-normalized volume change was approximately -0.57 Mm^3 km^{-2} (Table 3). Ninety-nine percent of net volume change was associated with continuous seagrass habitat which also had the highest area-normalized volume change of -0.57 Mm^3 km^{-2}. Between 2017 to 2019, this feature showed accretion with mean elevation change of 0.12 m and net volume change of -0.0002 Mm^3 (Tables 2 and 4). Area-normalized volume change was approximately 0.13 Mm^3 km^{-2}. More than 99% of net volume change was associated with continuous seagrass habitat which also had the highest area-normalized volume change of approximately 0.14 Mm^3 km^{-2}.
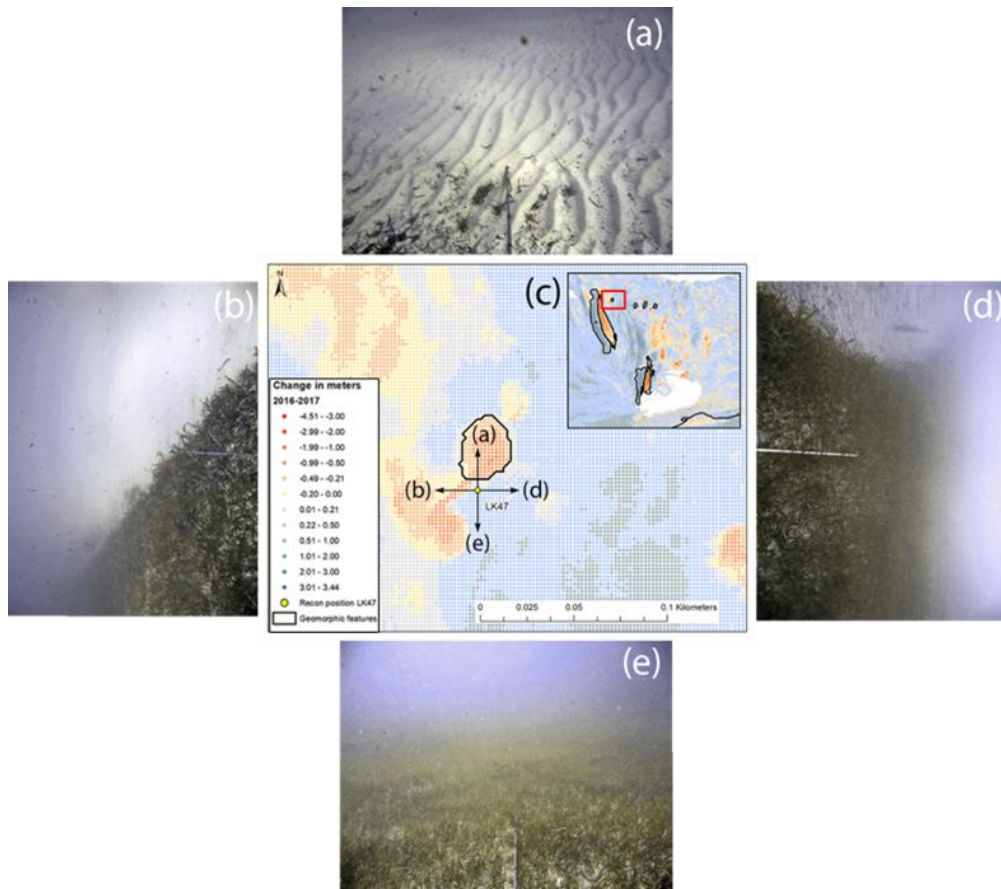
Figure 8. Cardinal orientation imagery (a, b, d, and e represent north, west, east, and south, respectively) and elevation change (c) at a scour mark location used to validate benthic features observed in elevation change data. East and west arrows show the boundaries between seagrass beds and sand flats in the elevation change data (c) and imagery (b and d). High erosion was noted between 2016 and 2017 on the sand flat (western) side of the habitat transition and minimal accretion was noted on the seagrass bed (eastern) side of the habitat transition. Photo credit: Mitch Lemon, Cherokee Nations System Solutions for U.S. Geological Survey.

3.2.3 Rubble Fields

Migration of reef rubble fields was observed in areas north and northeast of Looe Key Reef between 2016 and 2017. The largest of these features was approximately 418 m long and x 122 m wide at its widest point in 2017, 3 m in height from the crest to base on the deepest (western) edge, with average water depth of approximately 3.3 m (Fig 6g, h, and i). Transect elevation profiles showed the location of this feature in 2016, westward migration of approximately 80 m (crest to crest) in 2017, and minor eastward migration of 8 m (crest to crest) in 2019 (Fig. 7c). The accretion area of this feature covered an area of about 0.03 km^2 including approximately 43% reef rubble, 49% discontinuous seagrass, and 9% unconsolidated sediment. Between 2016 and 2017, mean elevation change of the accretion area (2017 location of the rubble field) was 0.89 m (Table 2) with a maximum elevation gain of 2.21 m. Total net volume change was 0.025 Mm^3 and area-normalized volume change was

0.914 Mm^3 km^{-2} with discontinuous seagrass accounting for 54% of net volume change indicating burial of seagrass during migration of the rubble field (Table 3). Highest mean elevation and area-normalized volume changes were also associated with discontinuous seagrass habitat. An area of erosion (0.023 km^2) was observed in 2017 at the original 2016 location of the rubble field that was approximately 428 m long and x 78 m wide including 58% reef rubble, 31% discontinuous seagrass, and 11% unconsolidated sediment. Mean elevation-change of the erosion area between 2016 and 2017 was -0.63 m (Table 2) with a maximum elevation loss of -2.11 m. Total net volume change was approximately -0.015 Mm^3 and area-normalized volume change was -0.661 Mm^3 km^{-2} with 69% of net volume change associated with reef rubble (Table 3). Highest mean elevation and area-normalized volume changes were also associated with reef rubble.

Between 2017 and 2019, the rubble field (accretion area) showed mean elevation change of -0.24 m, net volume change of -0.007 Mm^3, and area-normalized volume change of -0.248 Mm^3 km^{-2} (Tables 2 and 4). Discontinuous seagrass showed greatest loss in mean elevation and area-normalized volume change and accounted for 59% of net volume change. The adjacent erosion area (original 2016 location of the rubble field) showed a mean elevation change of -0.10 m (Table 2) with a maximum elevation loss of -0.52 m. Total net volume change was approximately -0.002 Mm^3 and area-normalized volume change was -0.103 Mm^3 km^{-2} with 53% of net volume change associated with discontinuous seagrass (Table 4). Highest mean elevation and area-normalized volume changes were also associated with discontinuous seagrass. Mean elevation and volume losses generally decreased with increasing mean habitat depth in the erosion area (Tables 2 and 4).

3.2.4 Sand Lobe

Substantial accretion was observed along a sand lobe located near the base of the fore-reef slope of Looe Key Reef between 2016 and 2017 (Fig. 6j, k, and l). This feature was approximately 1,383 m long and 344 m wide (approximately 0.27 km^2) at the widest point with an average water depth of approximately 11.9 m in 2017 and included only unconsolidated sediment habitat. Between 2016 and 2017, mean elevation change was 0.51 m (Table 2) with maximum gains in elevation up to 1.5 m along the southern (seaward) downslope section of this feature and maximum elevation losses of -0.58 m along the northern landward section, nearest to the base of the of the fore-reef slope (Fig. 7d). Total net volume change was 0.14 Mm^3 and area-normalized volume change was 0.51 Mm^3 km^{-2} (Table 3). Between 2017 and 2019, mean elevation change was -0.20 m with maximum elevation losses up to -1.12 m (Table 2, Fig. 7d). Only 852 of 67,389 elevation points analysed for this feature showed gains in elevation after 2017, averaging 0.05 m. Transect elevation profiles showed relatively consistent losses in elevation (erosion) across the sand lobe north to south (landward to seaward) during this time-period. Total net volume change was -0.05 Mm^3 and area-normalized volume change was -0.20 Mm^3 km^{-2} (Table 4).

4 Discussion

4.1 Storm Impacts

465 There are few comprehensive assessments of the effects of major hurricanes on seafloor elevation and geomorphology on coral reefs; and no quantitative studies of reef-scale seafloor elevation change resulting from tropical storm impacts have previously been conducted in the Florida Keys. Our results showed Hurricane Irma was primarily a depositional event that increased mean seafloor elevation and volume over a 15.98 km^2 section of Looe Key Reef by 0.34 m (annualized elevation-change rate of up to 247 mm yr^{-1}) and up to 5.4 Mm^3, respectively, with area-normalized volume change of approximately 0.34 Mm^{3}km^{-2}. Our

470 observations were based on elevation measurements collected 13.5 months before the storm and three to six months after the storm and, therefore, included any persistent change that occurred during quiescent sea state conditions before and after the passing of Irma. However, observations during several rapid reef assessments after the storm also indicated broad-scale sediment deposition as a direct result of Hurricane Irma (Viehman et al., 2018; Walker, 2018; Wilson et al., 2020; Kobelt et al. 2019), which corroborates our findings of increased mean elevation and sediment accretion resulting from this storm event.

475 Furthermore, wind conditions were relatively quiescent from the 2016 lidar acquisition date up to the passing of Hurricane Irma and after the storm.Historical aerial imagery of LKR from 2014 and 18 March 2017 (3 years and 6 months prior to Hurricane Irma, respectively, Fig. 9) shows that patterns of major sedimentary features were mostly static in the few years prior to the storm (Finkl and Vollmer, 2017), further suggesting that broad scale sediment deposition resulted directly from Hurricane Irma.

480

Numerical modelling of the impact of hurricane-induced wave-current interactions on the transport of material along the FRT during Hurricane Irma showed that wave radiation stress primarily affected particle transport trajectories during the passage of the hurricane (Dobbelaere et al., 2022). Additionally, wave energy dissipation occurred through depth-induced wave breaking and bottom dissipation at the shelf break and over the coral reefs. Our 2016 to 2017 elevation change results showed

485 general movement of sediment and migration of major geomorphic features from ENE to WSW in shallow areas of the reef proper and back reef area (ranging from approximately 2 to 5.5 m water depth in 2016), consistent with the direction of sustained, high magnitude winds and modelled particle transport trajectories during the passing of Hurricane Irma (Fig. 4; Fig. 6a, d, and g). For example, large sand waves and rubble fields (approximately 0.02 to 0.06 km^2 in area) migrated westward approximately 80 m (Fig. 6a and g) causing burial of seagrass habitat. Scour marks developed due to erosion of the western

490 edges of seagrass beds and westward transport of sediment, causing burial of adjacent seagrass beds between scour marks (Fig. 6d). Furthermore, numerical modelling showed that, after the passage of the hurricane, suspended particles were transported northeastward by the Florida Current and were advected (via Stokes drift) from the outer shelf to inshore for approximately 2 days (Dobbelaere et al., 2022), consistent with observations of sediment plumes that likely contributed to broadscale sediment deposition resulting from Hurricane Irma (Fig. 1d).

495
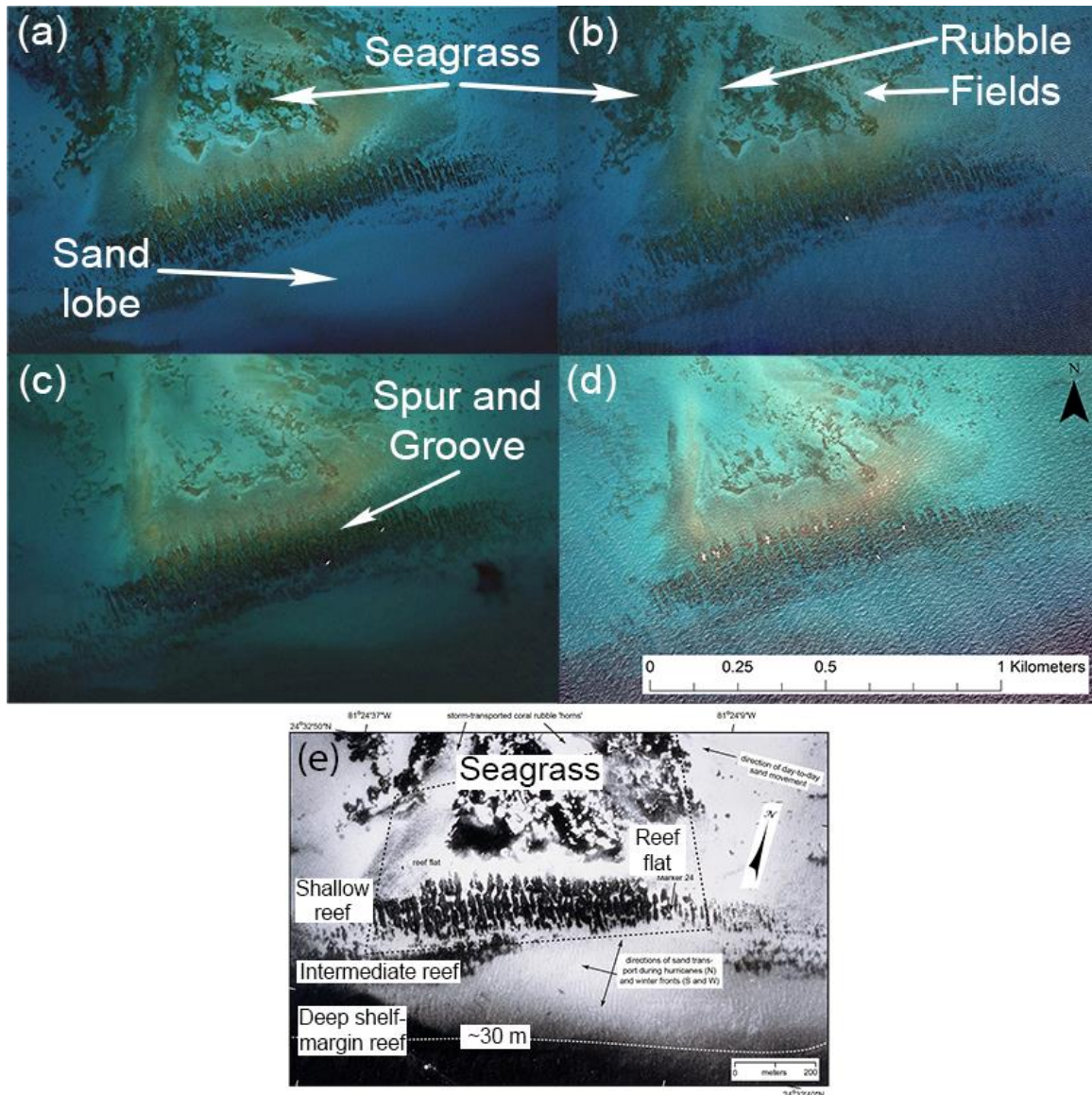
Figure 9. Historical satellite and aerial imagery of Looe Key Reef. Imagery from (a) 17 December 2014, before Hurricane Irma; (b) 18 March 2017, before Hurricane Irma; (c) 30 December 2017, 3 months after Hurricane Irma; (d) 2019, 16.5 months after Hurricane Irma; and (e) from 1975 (Lidz et al., 2016). Panels a, b, and c source: Maxar 2023 via Google Earth Pro 7.3.6.9345, downloaded 11 September 2023. Panel d source: 2019 NOAA National Geodetic Survey via NOAA Digital Coast, downloaded 11 September 2023, https://www.fisheries.noaa.gov/inport/item/63292.

Geomorphic seafloor changes, like those observed in our study, have been documented for other category 4 hurricanes in the Florida Keys based on photographic air and ground surveys, maps, sediment cores, and bottom markers. For example, in 1967, Hurricane Donna approached from the southeast and passed over the central islands of the Florida Keys in September 1960

with sustained winds of 226 km h^{-1} (category 4) and with breaking waves and storm currents causing broken coral rubble up to a meter in diameter, shoreward transport of gravel to boulder sized rubble and sand approximately 60 to 150 m shoreward, and burial of seagrass with 15 cm of sediment (Ball et al., 1967). Hurricane Betsy approached from the west and passed over the Florida Keys approximately 25 km north of Hurricane Donna's landfall in September 1965 with sustained winds of up to 226 km h^{-1}. While both storms had similar destructive effects to corals on the outer reefs, Hurricane Betsy produced less rubble, showed an overall effect of erosion and recycling of sediment in the environment, and caused sediment plumes from the mainland to the edge of the Gulf Stream for several days after the Hurricane passed (Perkins and Enos, 1968). Perkins and Enos (1968) noted the difference in wind directions for the two storms caused different effects, and that it is difficult to extrapolate quantitative sedimentation rates from the sedimentary record of one hurricane and frequency of recorded hurricanes. Hurricane Andrew made landfall along the southeast coast of Florida just south of Miami also with sustained winds of 226 km h^{-1} with maximum wave heights of less than 2 m. Branching corals were broken, massive coral heads were toppled, seafans and sponges were ripped loose, and shallow reefs sustained the most damage (Orr and Ogden, 1992); however, there was little damage to seagrass beds immediately seaward of coastal mangroves (Tilmant et al., 1994). Hurricane Georges was a category 2 storm that passed over Key West with maximum sustained winds of only 145 km h^{-1}. However, data from 30 seagrass monitoring transects showed a 3% decline in density of *Thalassia testudinum* and 19% decline in density of *Syringodium filiforme* seagrasses, with complete loss of seagrass beds at 3 monitoring stations, burial of one station with 50cm of sediment, and substantial erosion at two stations (Fourqurean and Rutten, 2004). Furthermore, Fourqurean and Rutten (2004) showed that seagrass recovery was slowest at sites that were eroded; losses by mechanical thinning and burial with only a few centimeters of sediment recovered quickly; and seagrass buried with 10s of centimeters of sediment hadn't recovered by three years after the storm. Analysis of long-term benthic monitoring stations in the FKNMS by Krause et al. (2023) showed some locations with substantial erosion of seagrass due to storm events that resulted in bare patches of seafloor or "blowouts" often larger than 20 m in diameter and similar to the scour marks observed in our study. Studies of post-storm seagrass recovery in other geographic locations indicate that revegetation of these large bare patches may take several years to multiple decades (Patriquin, 1975; Hastings et al., 1995; Kirkman and Kirkman, 2000; Carter et al., 2022). Results from these studies show the variability in storm impacts due complex interactions among factors such as location, fetch, wind speed, duration, storm history, and water depth (Fourqurean and Rutten, 2004), and demonstrate the value of comprehensive, quantitative post storm assessments of geological and ecological impacts.

Analysis of seafloor elevation change at LKR during the decade prior to Hurricane Irma (from 2004–2016, during which only one minor tropical storm impacted this location in 2008) indicated an increase in mean elevation of 0.39 m (annualized elevation-change rate of 32.5 mm yr^{-1}), net volume gain of up to 6.4 Mm^3 and area-normalized volume change of 0.39 Mm^3 km^{-2}, with accretion observed across all habitat types and some WSW movement of sand waves (Yates et al., 2019). Our results showed that sediment deposited during the approximately 16.5 to 19.5-month time-period including impacts from Hurricane Irma caused changes in seafloor elevation and volume across all habitat types similar in magnitude to net changes observed

over the past decade and at annualized elevation-change rates one order of magnitude greater (247 mm yr^{-1}). Previous studies on several coral reefs around St. Croix, U.S. Virgin Islands showed that storms can increase sediment transport by an order of magnitude higher than during non-storm conditions and that physical transport of sediment is primarily due to wave-induced oscillatory and unidirectional currents.(Hubbard et al., 1981; Hubbard, 1986). Measurements from 15 locations around St. Croix showed sediment transport rates ranging from 0.009 to 0.3 Mm^3 km^{-2}yr^{-1} during non-storm conditions, and 0.09 to 1.5 Mm^3 km^{-2}yr^{-1} during storm conditions (Hubbard et al., 1981; Yates et al., 2017). Similarly, sediment trap studies along the southwest coast of Puerto Rico showed median sediment accumulation rates increased by an order of magnitude (from approximately 6 to 68 mg m^{-2} d^{-1}) after the passage of Hurricane Maria in September of 2017 (a category 4 storm) and a large October 2017 storm that caused resuspension of bottom sediments (Takesue et al., 2021). Furthermore, these accumulation rates exceeded the threshold of 10 mg m^{-2} d^{-1} which is considered heavy sedimentation and has been associated with fewer coral species, less live coral, lower coral growth rates, reduced coral recruitment and calcification rates, and slower rates of reef accretion (Rogers, 1990).

Mean elevation- and area-normalized volume-change from 2016–2017 for habitats examined in our study increased significantly with water depth suggesting that, in addition to broad-scale sediment deposition across the study site, sediment was also transported from shallower to deeper habitats (Fig. 5a and b). Notably, greatest increases in elevation (accretion) were associated with habitats in water depths exceeding 11 m including aggregate reef, a sand lobe consisting of unconsolidated sediment, and 'not classified' habitat located seaward and near the base of the reef's spur-and-groove formation, suggesting some movement of sediment offshore and downslope (Fig. 4a, Table 2). Additionally, erosion was observed in the shallower, upslope grooves of the spur-and-groove formation, and accretion was observed in the deeper, downslope areas of the grooves from 2016 to 2017 further suggesting downslope, offshore movement of sediments (Fig. 10). The sand lobe at the base of the spur and groove formation also showed upslope erosion and considerable downslope (seaward) accretion, further suggesting offshore transport of sediments (Fig. 7d). Our observations are consistent with previous bathymetric change analyses conducted along the northern FRT from 2001 to 2008 (approximately 3 years before Hurricane Ivan and 3 years after Hurricane Katrina) that showed movement of up to 1.8 Mm^3 of sediment between these time periods and transport of sediment from the inner shelf to offshore and beyond the shelf edge through gaps in the barrier reef and diabathic (cross-shore) channels during high-energy events or when the back reef overfills with sand (Finkl, 2004; Finkl and Vollmer, 2017). These observations are also consistent with results of Yates et al. (2017) that show a multi-decadal trend along the FRT of reef sediment transport down the fore-reef-slope and export offshore.

Results from previous studies of sediment mobility along the FRT suggest that some sediment transport observed in our study could be due to persistent transport of sand during quiescent sea state conditions. Field observations of currents, waves, and reef sediment grain-size analyses coupled with integrated ocean-atmosphere-wave-sediment transport modelling during a one-year study at Crocker reef in the Upper Florida Keys showed that sediment mobility was primarily driven by wave stress

exceeding critical shear stress; current stress alone only exceeded the critical shear stress for sediment mobility 5% of the time usually due to Florida Current eddies (Torres-Garcia et al., 2018). Torres-Garcia et al. (2018) showed that nonbreaking wave stress (characteristic of quiescent sea states) mobilizes sand approximately 23 to 59% of the time; and fine-grained material is winnowed from the shallow areas of the reef and deposited to the flanks and offshore, particularly to the southwest. Southwest

580   counter currents due to the formation of Florida Current eddies (Lee and Williams, 1999) and WSW movement of sand wave features over a decadal time-period (Yates et al., 2019b) have also been observed near LKR. However, Torres-Garcia et al. (2018) also showed the critical stress threshold of gravel-sized material was exceeded 1 to 13% of the time, particularly during near-field tropical storm conditions (similar to Hurricane Wilma, a category 3 hurricane) that cause breaking waves, mobilize and transport gravel material, and can cause physical reef degradation. Their results, suggest the large volume of material

585   transported at Looe Key Reef (including gravel-sized and larger reef rubble) during the short time-period of our study from 2016 to 2017 was likely due primarily to storm conditions caused by Hurricane Irma.
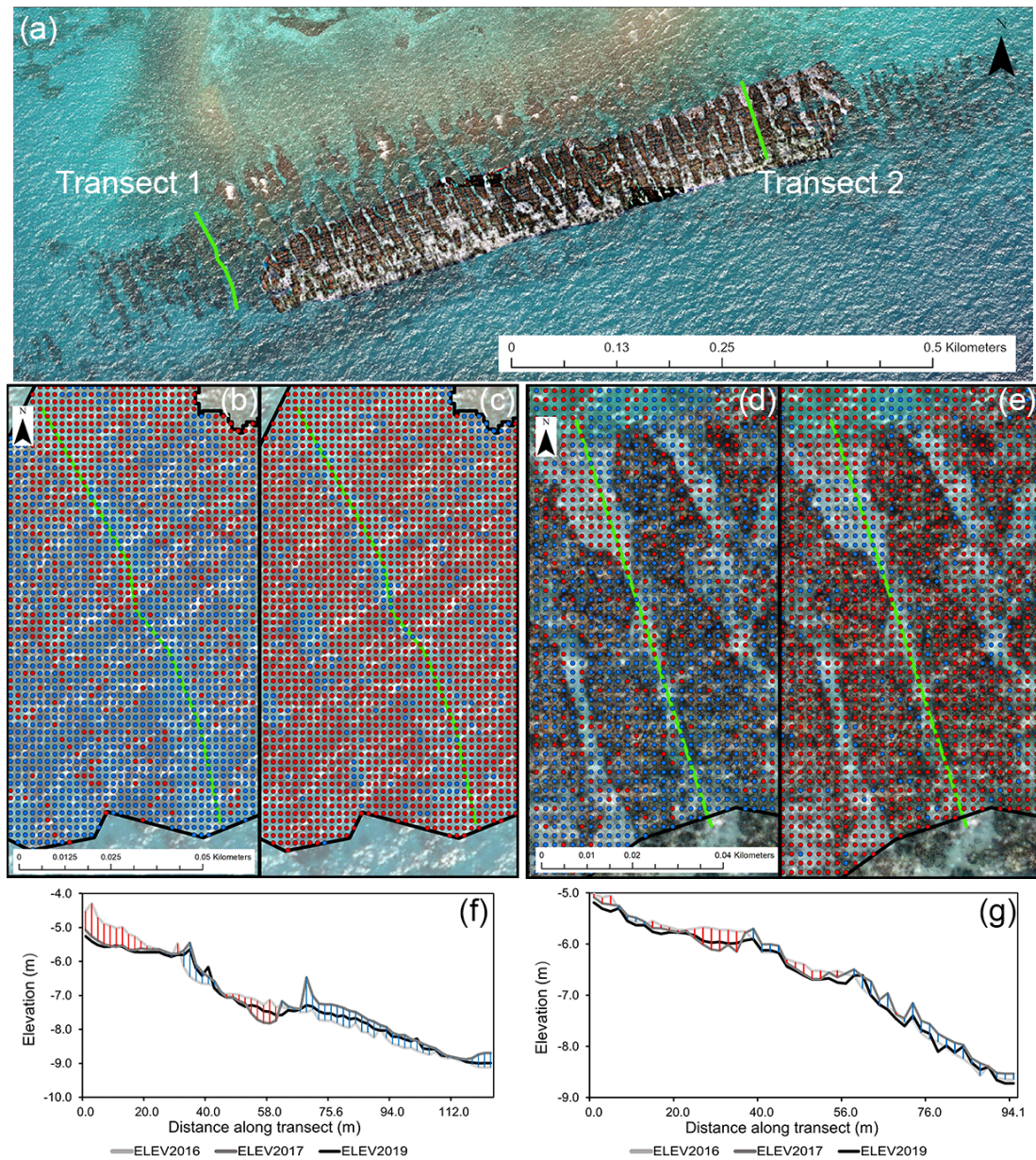
590 **Figure 10. Elevation-change along Looe Key Reef spur and groove formation.** (a) Upslope to downslope transects along Looe Key Reef spur and groove formation (green lines); image source: 2019 NOAA National Geodetic Survey via NOAA Digital Coast, downloaded 11 September 2023, https://www.fisheries.noaa.gov/inport/item/63292 with structure from motion overlay image of Hatcher et al. (2022). Areas of erosion (red circles) and accretion (blue circles) along transect 1 between (b) 2016 and 2017, and between (c) 2017 and 2019. Areas of erosion (red circles) and accretion (blue circles) along transect 2 between (d) 2016 and 2017, and between € 2017 and 2019.

595 Elevation profiles from 2016, 2017, and 2019 for (f) transect 1 and (g) transect 2. Vertical red lines indicate net erosion and vertical blue lines indicate net accretion between 2016 and 2017.

4.2 Post-storm Change

600 Approximately 16.5 months after Hurricane Irma (during a 13-month period between 2017 and 2019), decreased elevation was observed across all habitats with mean elevation-change of -0.15 m (annualized elevation change-rate of -139 mm yr^{-1}), net volume change up to -2.46 Mm^3, and area-normalized volume change of -0.15 Mm^{3}km^{-2} due to erosion. Newly deposited carbonate sediments typically have porosities of 40 to 70% (Choquette and Pray, 1970) at shallow sediment depths of a few hundreds of meters (Schmoker and Halley, 1982). Porosity of carbonate sands on the FRT and in Hawk Channel ranges from

605 60 to 72% in the upper 22 cm of deposited sediment (Walter et al., 2007). Schmoker and Halley (1982) showed that there is little or no sediment porosity loss at near-surface sediment depths. Application of their exponential function for porosity versus depth of sediment (porosity (%) = 41.73e$^{-z/2498}$, where z = depth below sediment surface) indicates that the decrease in porosity of deposited carbonate sediments at 2 m below the sediment-surface due to compaction is only 0.03%. Furthermore, carbonate sands have settling velocities ranging from 0.025 to 0.364 m s^{-1} (Riazi et al., 2020). Satellite imagery shows the sediment

610 plume caused by resuspension of sediment during Hurricane Irma cleared within approximately 5 days of the storm's passing (NASA, 2023). Therefore, it is likely that resuspended sediment settled quickly (within days) when storm conditions subsided; and compaction and loss of sediment porosity after the storm cannot account for the decrease in elevation observed at our study site between 2017 and 2019. This suggests that approximately 50% of sediment deposited between 2016 and 2017 was eroded by 2019 due to physical transport away from the study site.

615

Geomorphic features including the sand wave and reef rubble field showed continued erosion between 2017 to 2019 with some evidence for migration of the crest of the rubble field back toward its original 2016 position indicated in the elevation profile (Fig. 6 and 7). Shallow areas between the scour marks showed erosion, while the scour mark pits showed infilling (Fig. 6 and 7). Spurs of the spur-and-groove formation primarily showed erosion, while shallow (landward) sections of grooves showed

620 some accretion, likely due to transport of sediments from spurs to grooves and downslope from the shallow reef (Fig. 10). Deeper (seaward) areas of grooves and the sand lobe located at the base of the spur and groove formation showed erosion (Fig. 4 and 6k) suggesting continued downslope, offshore transport of sediments. Historical aerial and satellite imagery from before and after the passing of Hurricane Irma corroborates our elevation-change observations (Fig. 9). Imagery from 2014 and March 2017 shows that major geomorphic features of Looe Key proper such as distribution of seagrass beds and the size and position

625 of the sand lobe and rubble fields were relatively static between these time periods leading up to Hurricane Irma (Fig. 9a and b). Imagery from December 2017, three months after Hurricane Irma passed, shows broad scale sediment deposition and burial of seagrass beds in the shallow areas of the reef proper, erosion and exposure of deeper, downslope spur-and-groove formation and downslope deposition on the sand lobe (Fig. 9c). Imagery from 2019 shows re-exposure of some shallow seagrass beds and deep spur-and-groove formation as sediments were eroded (Fig. 9d). Historical aerial imagery from 1975 (Fig. 9e, Lidz et

630 al., 2016) shows a distribution of seagrass, presence of rubble fields, and patterns of sediment along the sand lobe similar to 2014 and 2017 imagery (before Hurricane Irma) indicating these features have persisted over the past several decades despite

repeated impact from tropical and seasonal storms. Lidz et al. (2016) suggested the formation of rubble fields in the shallow back reef area is mainly due to historical passage of hurricanes and winter storms, and our elevation change results suggest that these structures continue to migrate in response to storm conditions. Lidz et al. (2016) also suggested that transport of sediment during hurricanes was primarily to the north. Our observations showed primary sediment movement during Hurricane Irma was WSW and downslope from shallow to deep habitats with apparent seaward movement of the sand lobe after the storm passed, illustrating the variability in storm impacts associated with individual storm events.

Previous examination of multi-decadal elevation-change in a 19 km^2 study site at Looe Key Reef from 1938 to 2004 showed mean elevation change of -0.30 m (annualized elevation-change rate of -4.5 mm yr^{-1}), net volume loss up to -5.7 Mm^3, and area-normalized volume change of -0.30 Mm^3 km^{-2} indicating a long-term trend of erosion at this location over more than six decades (Yates et al., 2017). Similar results were observed for a 241 km^2 area of the Upper Florida Keys with an annualized elevation-change rate of -1.4 mm yr^{-1} between 1934 and 2004 (Yates et al., 2017). Furthermore, six of nine habitats at LKR showed elevation loss over those periods, with greatest losses associated with shallow habitats, and mean elevation and volume gains in deep-water habitats including at the base of the spur-and-groove habitat, indicating transport of reef sediments down the fore-reef-slope and export offshore (Yates et al., 2017). Our observed rate of mean elevation loss between 2017 and 2019 (-139 mm yr^{-1}) was two orders of magnitude higher than the multi-decadal rates of Yates et al. (2017). Additionally, elevation loss (erosion) showed a moderate correlation with water depth, and mean elevation losses during 2017 to 2019 were significantly greater in habitats with larger mean elevation gains during 2016 to 2017, suggesting that sediment distribution was re-equilibrating or stabilizing to quiescent sea-state conditions up to 16.5 months after the storm.

The annualized mean rate of elevation-change for LKR from the 2.5-year period between July 2016 to January 2019 examined in our study, including sediment accretion from Hurricane Irma and the post-storm erosion and re-equilibration, was approximately 72 mm yr^{-1}, which is almost double the rate of accretion observed in the previous decade of 32.5 mm yr^{-1} (Yates et al. 2019b). Numerous field reconnaissance observations immediately after the passing of Hurricane Irma indicated broadscale sediment deposition across the FRT due to the storm (e.g., Viehman et al., 2018; Walker, 2018; Wilson et al., 2020; Kobelt et al., 2019). Our 2016 to 2019 elevation-change rate is consistent with annualized mean elevation-change rates from 2016 to 2019 for the Lower FRT from approximately Big Pine Key to Key West of 84 mm yr^{-1}, and for the FRT from Miami to Key West of 76 mm yr^{-1} (Fehr et al., 2021), further suggesting that sediment distribution may have still been undergoing post-storm re-equilibration at our study site and along the broader FRT (Table 5).

Collection and analysis of additional elevation-change data sets over shorter time-periods (e.g., seasonal to annual) could improve characterization of post-storm elevation-change rates and duration of post-storm sediment re-equilibration periods relative to persistent seasonal, interannual, decadal, and multi-decadal time periods. Our results also suggest that caution should be used in selection of DEMs for use in elevation change and projection modelling to minimize bias that could result from

selecting elevation surfaces that reflect periods of rapid elevation change due to storm impacts and periods of post-storm re-equilibration.

Table 5. Annualized mean elevation-change rates (mm yr^{-1}) for event-driven to multi-decadal time periods at the Florida Keys Reef Tract.

| Location | Annualized mean elevation change rate (mm yr^{-1}) | | | | |
	Event-driven[a] 2016 to 2017	Post-storm[b] 2017 to 2019	Short-term[c] 2016 to 2019	Decadal 2004 to 2016	Multi-decadal 1930s to 2000s
Looe Key Reef	247	-139	72	32.5[d]	-4.5[e]
Lower Florida Reef Tract (south of Big Pine)	na	na	84[f]	na	na
Florida Reef Tract (Miami to Key West)	na	na	76[f]	na	na
Upper Florida Reef Tract (Elliott Key to Tavernier Key)	na	na	na	na	-1.4[e]

a = calculated assuming a total time-period of 16.5 months (13.5 month pre- to 3 months post-storm); b = total time period 13.5 months (3 to 16.5 months post-storm); c = total time-period approximately 30 months (13.5 months pre- to 16.5 months post-storm); d = using data from Yates et al., 2019; e = using data from Yates et al., 2017; f = using data from Fehr et al., 2021; na = no data available.

5 Conclusion

High-resolution lidar and multibeam bathymetric data were used to quantify seafloor elevation and volume change within the Looe Key Reef system of the Florida Keys Reef Tract over a 2.5-year period from 2016–2019 and to examine impacts from category-4 Hurricane Irma and post-storm re-equilibration of seafloor sediments. Analysis of seafloor elevation and volume change over a 16.5-month period from July 2016 to December 2017 showed Hurricane Irma caused broadscale deposition of sediments across all benthic habitats of this reef system and burial of seagrass and coral dominated habitat. Rates of net elevation change were one order of magnitude greater during this short-term period that included storm impacts from Hurricane Irma than for the previous decade (Yates et al., 2019). Major seafloor geomorphic features such as sand waves and rubble fields migrated 10s of meters to the WSW in response to predominant wind conditions during the passing of Hurricane Irma, and sediment accretion was significantly greater in deep habitats than shallow habitats, suggesting downslope and offshore transport of seafloor sediment.

Loss of mean elevation and volume in all habitats in the period following the storm (from December 2017 to January 2019) indicated that 35% to 50% of sediment deposited during the storm had eroded by approximately 16.5 months after the storm and that erosion rates were two orders of magnitude greater than historical, multi-decadal rates of erosion. Sediment erosion after the storm (2017–2019) was moderately correlated with depth and was significantly greater in habitats that showed greater accumulation during the period including Hurricane Irma from 2016–2017, suggesting a period of rapid sediment re-equilibration after the storm. Historical satellite and aerial imagery show that major geomorphic features at this location including rubble fields, sand waves, and a sand lobe at the base of the spur-and-groove formation have persisted over the past several decades despite impacts from storms. However, our elevation-change results indicate these features are highly

ephemeral, migrating rapidly during storms, re-equilibrating to non-storm sea state conditions between storms, and periodically

695 burying seafloor habitat such as seagrass. Such features and the area surrounding them likely represent localized areas of long- and short-term seafloor instability that could be less suitable for restoration of slow growing benthic species. Our observed rates of elevation change in the 16-month period after Hurricane Irma were one to two orders of magnitude greater than during the past decade or multi-decadal period (Yates et al., 2017; 2019b) indicating seafloor sediments across all habitats may have still been re-equilibrating to non-storm sea state conditions up January 2019. Higher resolution elevation-change data collected

700 over seasonal and annual time periods could improve characterization and understanding of short-term (event-driven, seasonal, interannual) and long-term (decadal to multi-decadal) rates and processes of seafloor change and help guide benthic habitat post-storm recovery and restoration efforts in topographically complex coral reef systems.

Code availability

705 Python script for the Seafloor Elevation Change Analysis Tool (SECAT), intended to be applied in ArcMap or ArcGIS Pro, is publicly available as a U. S. Geological Survey software release, doi: 10.5066/P9D5UUZ0, https://www.usgs.gov/software/seafloor-elevation-change-analysis-tool.

710 **Data availability**

Elevation-change and multibeam bathymetric data are publicly available in U.S. Geological Survey Data Releases at https://doi.org/10.5066/P9CHC95D, https://doi.org/10.5066/P937LNZF, https://doi.org/10.5066/P9NXNX61, https://doi.org/10.5066/P9JTOOMB and https://doi.org/10.5066/P9P2V7L0. Lidar topobathymetric data are publicly available from the NOAA Office for Coastal Management at https://www.fisheries.noaa.gov/inport/item/63018 and

715 https://www.fisheries.noaa.gov/inport/item/48373. Seafloor habitat data are publicly available from the Florida Fish and Wildlife Conservation Commission, Fish and Wildlife Research Institute at http://ocean.floridamarine.org/IntegratedReefMap/UnifiedReefTract.htm.

Author contribution

720 KY and DZ conceptualized the research, data acquisition approach, and methodology for analysis of seafloor elevation data. KY, ZF, and DZ performed formal analysis of data. DZ developed the SECAT software for statistical analysis of elevation- and volume-change data. KY and ZF developed data interpretations and prepared the original manuscript draft with contributions from SJ and DZ. All authors contributed to preparation of the final, published manuscript.

725 **Competing interests**

The authors declare that they have no conflict of interest.

Disclaimer

Any use of trade, firm, or product names is for descriptive purposes only and does not imply endorsement by the U.S.
730   Government.

Acknowledgement

Funding for this study was provided by the U.S. Geological Survey, Coastal and Marine Hazards and Resources Program and
by 2018 Hurricane and Wildfire Supplemental Funding provided to the U.S. Geological Survey from the Additional
735   Supplemental Appropriations for Disaster Relief Requirements Act of 2018 (P.L. 115-123). We would like to thank J.J.
Fredericks, B.J. Reynolds, and A.S. Farmer for collection of the multibeam bathymetry data and J.J. Fredericks for
development of the associated multibeam digital elevation model. We also thank J. Zieg for assistance with development of
the SECAT software and K. Murphy for assistance with development of methods for sub-sampling large-scale digital elevation
models. We greatly appreciate reviews of the original draft manuscript and constructive comments from L. Toth and G.
740   Hatcher.

References

Awadallah, M.O.M., Malmquist, C., Stickler, M., and Alfredsen, K.: Quantitative evaluation of bathymetric LiDAR sensors
and acquisition approaches in Lærdal River in Norway, Remote Sens., 15, 263, https://doi.org/10.3390/rs15010263, 2023.
745   Ball, M. M., Shinn, E. A., and Stockman, K. W.: The geologic effects of Hurricane Donna in south Florida, J. Geol., 75, 583–
597, 1967.

Bhatia, K. T., Vecchi, G. A., Knutson, T. R., Murakami, H., Kossin, J., Dixon, K. W., and Whitlock, C. E.: Recent increases
in tropical cyclone intensification rates, Nat. Commun., 10, 1–9, https://doi.org/10.1038/s41467-019-08471-z, 2019.
750

Bohnsack, J. A., Cantillo, A. Y., and Bello, M. J.: Resource survey of Looe Key National Marine Sanctuary 1983, NOAA
Technical Memorandum, NOS NCCOS CCMA 160, NMFS-SEFSC-478, NOAA LISD Current References 2002–8,
https://www.aoml.noaa.gov/general/lib/CEDAR_files/cedar106.pdf, 2002.

755   Brandt, M.E. and McManus, J.W.: Disease incidence is related to bleaching extent in reef building corals, Ecology 90(10),
2859–2867, https://doi.org/10.1890/08-0445.1, 2009.

Bruno, J. F., Sweatman, H., Precht, W. F., Selig, E. R., Virginia, and Schutte, V. G. W.: Assessing evidence of phase shifts
from coral to macroalgal dominance on coral reefs, Ecology, 9, 1478–1484, https://doi.org/10.1890/08-1781.1, 2009.
760

Cangialosi, J. P., Latto, A. S., and Berg, R.: National Hurricane Center tropical cyclone report Hurricane Irma (AL112017) 24 September 2021, Tropical Cyclone Report, AL112017, https://www.nhc.noaa.gov/data/tcr/AL112017_Irma.pdf, 2021.

765 Carter, A. B., Collier, C., Coles, R., Lawrence, E., and Rasheed, M. A.: Community-specific "desired" states for seagrasses through cycles of loss and recovery, J. Environ. Manage., 314, 115059. https:// doi. org/ 10. 1016/j. jenvm an. 2022. 115059, 2022.

Choquette, P. W., and Pray, L. C.: Geologic nomenclature and classification of porosity in sedimentary carbonates, AAPG Bull., 54, 207–250, https://doi.org/10.1306/5D25C98B-16C1-11D7-8645000102C1865D, 1970.

770

Dobbelaere, T., Curcic, M., Henaff, M.L., and Hanert, E.: Impacts of Hurricane Irma (2017) on wave-induced ocean transport processes, Ocean Model., 171, 1–13, https://doi.org/10.1016/j.ocemod.2022.101947, 2022.

Elsner, J. B., Kossin, J. P., and Jagger, T. H.: The increasing intensity of the strongest tropical cyclones, Nature, 455, 92–95, 775 https://doi.org/10.1038/nature07234, 2008.

Fehr, Z. F., and Yates, K. K.: Underwater photographic reconnaissance and habitat data collection in the Florida Keys–a procedure for ground truthing remotely sensed bathymetric data, USGS Open-File Report, 2020–1118, 13 pp., https://doi.org/10.3133/ofr20201118, 2020.

780

Fehr, Z.W., Zawada, D.G., and Yates, K.K.: Seafloor elevation and volume change analyses from 2016 to 2019 along the Florida Reef Tract, USA, U.S. Geological Survey data release, USGS [data set], https://doi.org/10.5066/P9CHC95D, 2021.

Fernandez-Diaz, J.C., Glennie, C.L., Carter, W.E., Shrestha, R.L., Sartori, M.P., Singhania, A., Legleiter, C.J., Overstreet, 785 B.T.: Early results of simultaneous terrain and shallow water bathymetry mapping using a single-wavelength airborne LiDAR sensor, IEEE J. Sel. Top. Appl. Earth Obs. Remote Sens., 7, 623–635, https://ieeexplore.ieee.org/document/6542744, 2014. Ferrario, F., Beck, M.W., Storlazzi, C.D., Miheli, F., Shepard, C.C., and Airoldi, L.: The effectiveness of coral reefs for coastal hazard risk reduction and adaption, Nat. Commun., 5, 3794, doi:10.1038/ncomms4794, 2014.

790 Finkl, C.W.: Leaky valves in the littoral sediment budgets: loss of nearshore sand to deep offshore zones via chutes in barrier reef systems, southeast coast of Florida, USA, J. Coast. Res., 20, 605–611, https://doi.org/10.2112/1551-5036(2004)020[0605:LVILSB]2.0.CO;2, 2004.

Finkl, C. W., and Andrews, J. L.: Shelf geomorphology along the southeast Florida Atlantic continental platform: Barrier

795   coral reefs, nearshore bedrock, and morphosedimentary features, J. Coast. Res., 244, 823–849, doi:10.2112/08A-0001.1, 2008.

Finkl, C.W. and Vollmer, H.M.: Methods for investigating sediment flux under high-energy conditions on the Southeast Florida continental shelf using laser airborne depth sounding (LADS) in a geographic information system (GIS) dataframe, J.

800   Coast. Res., 33, 452–462, https://doi.org/10.2112/JCOASTRES-D-16A-00014.1, 2017.

Florida Department of Environmental Protection: Florida's coral reefs, https://floridadep.gov/rcp/rcp/content/floridas-coral-reefs#:~:text=Florida%20is%20the%20only%20state,spiny%20lobster%2C%20snapper%20and%20grouper, last access: 7 September 2023, 2023.

805

Florida Fish and Wildlife Conservation Commission-Fish and Wildlife Research Institute, Unified Florida Coral Reef Tract Map v2.0, FWC-FWRI [data set], http://ocean.floridamarine.org/IntegratedReefMap/UnifiedReefTract.htm, 2015.

Florida Reef Resilience Program. In Florida Reef Resilience Program Disturbance Response Monitoring and Hurricane Irma

810   Rapid Reef Assessment Quick Look Report: Summer 2017, https://repository.library.noaa.gov/view/noaa/15575, last access: 28 November 2021, 2017.

Fredericks, J. J., Reynolds, B. J., Farmer, A. S., Yates, K. K., and Zawada, D. G.: Multibeam bathymetry data collected in December 2017, February and March 2018 at Looe Key, the Florida Keys, U.S. Geological Survey data release, USGS [data

815   set], https://doi.org/10.5066/P9P2V7L0, 2019.

Fourqurean, J. W. and Rutten, L. M.: The impact of Hurricane Georges on soft-bottom, back reef communities: site-and species-specific effects in south Florida seagrass beds, B. Mar. Sci., 75, 239–257, 2004.

820   Gorstein, M., Dillard, M. K., Loerzel, J., Edwards, P. E. T., and Levine, A S.: National coral reef monitoring program socioeconomic monitoring component: summary findings for South Florida, NOAA Technical Memorandum, CRCP 25, doi: 10.7289/V5VH5KV5, 2014.

Hall, M. O., Furman, B. T., Merello, M., and Durako, M. J.: Recurrence of *Thalassia testudnum* seagrass die-off in Florida

825   Bay, USA: initial observations, Mar. Ecol. Prog. Ser., 560, 243–249, doi: 10.3354/meps11923, 2016.

Hall, E. R., Wickes, L., Burnett, L. E., Scott, G. I., Hernandez, D., Yates, K. K., Barbero, L., Reimer, J., Baalousha, M., Bennett-Mintz, J., Cai, W. J., Craig, K., Devoe, M. R., Fisher, W. S., Hathaway, T. K., Jewett, E. B., Johnson, Z., Keener, P., Mordecai, R. S., Noakes, S., Phillips, C., Sandifer, P. A., Schnetzer, A., and Styron J.: Acidification in the U.S. Southeast: causes, potential consequences and the role of the Southeast Ocean and Coastal Acidification Network, Front. Mar. Sci., 7, 548, doi: 10.3389/fmars.2020.00548, 2020.

Hastings, K., Hesp, P. and Kendrick, G. A.: Seagrass loss associated with boat moorings at Rottnest Island, Western Australia. Ocean & Coastal Management, 26, 225–246, https:// doi. org/ 10.1016/ 0964- 5691(95) 00012-Q, 1995.

Hatcher, G. A., Kranenbug, C. J., Warrick, J. A., Bosse, S. T., Zawada, D. G., Yates, K. K., and Johnson, S. A.: Overlapping seabed images and location data acquired using the SQUID-5 system at Looe Key, Florida, in July 2021, with structure-from-motion derived point cloud, digital elevation model and orthomosaic of submerged topography, U.S. Geological Survey data release, USGS [data set], http://doi.org/10.5066/P9WSF09G, 2022.

Hughes, T. P.: Catastrophes, phase shifts, and large-scale degradation of Caribbean coral reef, Science, 265, 1547–1551, https://doi.org/10.1126/science.265.5178.1547, 1994.

Hughes, T. P., Kerry, J. T., Álvarez-Noriega, M., Álvarez-Romero, J. G., Anderson, K. D., Baird, A. H., Babcock, R. C., Beger, M., Bellwood, D. R., Berkelmans, R., Bridge, T. C., Butler, I. R., Byrne, M., Cantin, N. E., Comeau, S., Connolly, S. R., Cumming, G. S., Dalton, S. J., Diaz-Pulido, G, Eakin, C. M., Figueira, W. F., Gilmour, J. P., Harrison, H. B., Heron, S. F., Hoey, A. S., Hobbs, J. A., Hoogenboom, M. O., Kennedy, E. V., Kuo, C., Lough, J. M., Lowe, R. J., Liu, G., McCulloch, M. T., Malcolm, H. A., McWilliam, M. J., Pandolfi, J. M., Pears, R. J., Pratchett, M. S., Schoepf, V., Simpson, T., Skirving, W. J., Sommer, B., Torda, G., Wachenfeld, D. R., Willis, B. L., and Wilson, S. K.: Global warming and recurrent mass bleaching of corals, Nature, 543, 373–377, doi: 10.1038/nature21707, 2017.

Jackson, J., Donovan, M., Cramer, K., and Lam, V. (Eds.): Status and trends of Caribbean coral reefs: 1970–2012, Global Coral Reef Monitoring Network, IUCN, Gland, Switzerland, 306 pp., https://www.iucn.org/content/status-and-trends-caribbean-coral-reefs-1970-2012, 2014.

Joyner, J. L., Sutherland, K. P., Kemp, D. W., Berry, B., Griffin, A., Porter, J. W., Amador, M. H., Noren, H. K., and Lipp, E. K.: Systematic analysis of white pox disease in *Acropora palmata* in the Florida Keys and role of *Serratia marcescens*, Appl. Environ. Microb., 81, 4451–4457, doi: 10.1128/AEM.00116-15, 2015.

860   Keller, B., Donahue, S., and Florida Keys National Marine Sanctuary U.S. Environmental Protection Agency State of Florida 2002—03 Sanctuary Science Report: An Ecosystem Report Card. In U.S. Department of Commerce, National Oceanic and Atmospheric Administration, National Ocean Service, Office of National Marine Sanctuaries, Florida Keys National Marine Sanctuary, Marathon, FL; 2006. Available online: http://sanctuaries.noaa.gov/science/conservation/pdfs/Keller1.pdf (accessed on 28 November 2021).

865

Kinzel, P.J., Wright, C.W., Nelson, J.M., and Burman, A.R: Evaluation of an experimental LiDAR for surveying a shallow, braided, sand-bedded river, J. Hydraul. Eng., 133, 838–842, https://doi.org/10.1061/(ASCE)0733-9429(2007)133:7(838), 2007.

870   Kirkman, H. and Kirkman, J.: Long-term seagrass meadow monitoring near Perth, Western Australia, Aquat. Bot., 67, 319–332, https:// doi. org/ 10. 1016/ S0304- 3770(00) 00097-8, 2000.

Knowlton, N.: Thresholds and multiple stable states in coral reef community dynamics, Am. Zoo., 32, 674–682, https://doi.org/10.1093/icb/32.6.674, 1992.

875

Knowlton, N.: The future of coral reefs, Proc. Natl. Acad. Sci. U.S.A., 98, 5419–5425, doi: 10.1073/pnas.091092998, 2001.

Knutson, T., Camargo, S. J., Chan, J. C., Emanuel, K., Ho, C.-H., Kossin, J., Mohapatra, M., Satoh, M., Sugi, M., Walsh, K. and Wu, L.: Tropical cyclones and climate change assessment: Part II: Projected response to anthropogenic warming, Bull.
880   Am. Meteorol. Soc., 101, E303–E322, https://doi.org/10.1016/j.tcrr.2020.01.004, 2020.

Kobelt, J. N., Sharp, W. C., Miles, T. N, and Feehan, C. J.: Localized Impacts of Hurricane Irma on Diadema antillarum and Coral Reef Community Structure, Estuar. Coast., 43, 1133–1143, https://doi.org/10.1007/s12237-019-00665-4, 2020.

885   Krause, J. R., Lopes, C. C., Wilson, S. S., Boyer, J. N., Briceño, H. O., Fourqurean, J. W.: Status and trajectories of soft-bottom benthic communities of the South Florida Seascape revealed by 25 years of seagrass and water quality monitoring data, Estuar. Coast., 46, 477-493, https://doi.org/10.1007/s12237-022-01158-7, 2023.

Krediet, C. J., Ritchie, K. B., and Teplitski, M.: The importance and status of Florida coral reefs; questions and answers,
890   University of Florida Institute of Food and Agricultural Sciences, 2009.

Kuffner, I. B., Lidz, B. H., Hudson, J. H., and Anderson, J. S.: A century of ocean warming on Florida Keys coral reefs: historic *in situ* observations, Estuar. Coast., 38, 1085–1096, doi:10.1007/s12237-014-9875-5, 2015.

895 Lapointe B. E. and Clark, M. W.: Nutrient inputs from the watershed and coastal eutrophication in the Florida Keys, Estuaries, 15, 465–476, doi:10.2307/1352391, 1992.

Lee, T. N. and Williams, E.: Mean distribution and seasonal variability of coastal currents and temperature in the Florida Keys with implications for larval recruitment, B. Mar. Sci., 64, 35–56,
900 https://www.ingentaconnect.com/contentone/umrsmas/bullmar/1999/00000064/00000001/art00005, 1999.

Legleiter, C.J., Overstreet, B.T., Glennie, C.L., Pan, Z., Fernandez-Diaz, J.C., and Singhania, A: Evaluating the capabilities of the CASI hyperspectral imaging system and Aquarius bathymetric LiDAR for measuring channel morphology in two distinct river environments, Earth Surf. Process. Landf., 41, 344–363, https://onlinelibrary.wiley.com/doi/10.1002/esp.3794,
905 2016.

Lessios, H. A., Cubit, J. D., Robertson, D. R., Shulman, M. J., Parker, M. R., Garrity, S. D., and Levings, S. C.: Mass mortality of *Diadema antillarum* on the Caribbean coast of Panama, Coral Reefs, 3, 173–182, doi: 10.1007/BF00288252, 1984.

910 Lidz, B. H., Reich C. D., and Shinn, E. A.: Regional Quaternary submarine geomorphology in the Florida Keys, GSA Bulletin, 115(7), 845-866, https://doi.org/10.1130/0016-7606(2003)115<0845:RQSGIT>2.0.CO;2, 2003.

Lidz, B. H., Reich, C. D., and Shinn, E. A.: Systematic mapping of bedrock and habitats along the Florida Reef Tract–Central Key Largo to Halfmoon Shoal (Gulf of Mexico), USGS Professional Paper, 1751, doi:10:3133/pp1751, 2016.
915

Littler, M. M., Littler, D. S., and Lapointe, B. E.: Baseline studies of herbivory and eutrophication on dominant reef communities of Looe Key National Marine Sanctuary, NOAA Technical Memorandum, NOS MEMD 1, https://repository.library.noaa.gov/view/noaa/2424, 1986.
Lohr, K. E., Ripple, K., and Patterson, J. T.: Differential disturbance effects and phenotypic plasticity among outplanted corals
920 at patch and fore reef sites, J. Nat. Conserv., 55, 1–7, https://doi.org/10.1016/j.jnc.2020.125827, 2020.

Malmstadt, J., Scheitlin, K., and Elsner, J.: Florida hurricanes and damage costs, Southeastern Geographer, 49, 108–131, http://www.jstor.org/stable/26225556, 2009.

925 Miller, M., Bourque, A., and Bohnsack, J.: An analysis of the loss of acroporid corals at Looe Key, Florida, USA: 1983–2000, Coral Reefs, 21, 179–182, doi: 10.1007/s00338-002-0228-7, 2002.

Moberg, F. and Folke, C.: Ecological goods and services of coral reef ecosystems, Ecol. Econ., 29, 215–233, doi: 10.1016/S0921-8099(99)00009-9, 1999.

930

Morris, J.T., Enochs, I.C., Besemer, N., Viehman, T.S., Groves, S.H., Blondeau, J., Ames, C., Towle, E.K., Grove, L.J.W., and Manzello, D.P.: Low net carbonate accretion characterizes Florida's coral reef. Sci. Rep. 12, 19582, https://doi.org/10.1038/s41598-022-23394-4, 2022.

935 Muehllehner, N., Langdon C., Venti, A., and Kadko, D.: Dynamics of carbonate chemistry, production, and calcification of the Florida Reef Tract (2009–2010): evidence for seasonal dissolution, Global Biogeochem. Cy., 30, 661–688, doi: 10.1002/2015GB005327, 2016.

Muller, E.M. and van Woesik, R.: Caribbean coral diseases: primary transmission or secondary infection?, Global Change
940 Biology, 1-7, doi: 10.1111/gcb.12019, 2012.

Mumby, P. J.: The impacts of exploiting grazers (Scaridae) on the dynamics of Caribbean coral reefs, Ecol. Appl., 16, 747–769, doi:10.1890/1051-0761(2006)016[0747:TIOEGS]2.0.CO;2, 2006.

945 Murphy, K. A., Zawada, D. G., & Yates, K. K. Subsampling Large-Scale Digital Elevation Models to Expedite Geospatial Analyses in Coastal Regions, J. Coastal Res., 38, 1236-1245, https://doi.org/10.2112/JCOASTRES-D-22-00015.1, 2022.

NASA: National Aeronautics and Space Administration, Earth Observing System and Information System (EOSDIS), Worldview Imagery, https://worldview.earthdata.nasa.gov/?v=-87.91450071116984,21.808851337497266,-
950 73.74396320747232,28.130239552037338&t=2017-09-13-T14%3A29%3A26Z, last access 2023.

National Geodetic Survey: 2018-2019 NOAA NGS Topobathy Lidar DEM Hurricane Irma: Miami to Marquesas Keys, FL, NOAA Office for Coastal Management [data set], https://www.fisheries.noaa.gov/inport/item/63018, 2022.

955 NHC: National Oceanic and Atmospheric Administration, National Hurricane Center: NOAA NHC – Irma storm track – best track + advisories, doi:10.4211/hs.aa5c9982a4694a19be2fa9299b78e5ca, 2018.

NOAA: National Oceanic and Atmospheric Administration, National Ocean Service, Office for Coastal Management, Digital Coast – Historical Hurricane Tracks, https://www.coast.noaa.gov/hurricanes/#map=4/32/-80, last access: 2022a.

960

NOAA: National Oceanic and Atmospheric Administration, National Weather Service, Detailed meteorological summary on Hurricane Irma, technical summary, https://www.weather.gov/tae/Irma_technical_summary, last access: 2022b, 2021.

NOAA Fisheries: Restoring seven iconic reefs: a mission to recover the coral reefs of the Florida Keys.

965   https://media.fisheries.noaa.gov/dam-migration/restoring_seven_iconic_reefs_-
      _a_mission_to_recover_the_coral_reefs_of_the_florida_keys.pdf, last access 26 January 2023, 2022.

NOAA-NOS. National Oceanic and Atmospheric Administration - National Ocean Service, Tides and Currents Station 8723970, https://tidesandcurrents.noaa.gov/stationhome.html?id=8723970, last access: 7 September 2023, 2023.

970

Norström, A. V., Nyström, M., Lokrantz, J., and Folke, C.: Alternative states of coral reefs: beyond coral–macroalgae shifts, Mar. Ecol. Prog. Ser., 376, 295–306, 2009.

Office for Coastal Management: 2016 NOAA NGS Topobathy Lidar DEM: Florida Keys Outer Reef Block 01, NOAA Office

975   for Coastal Management [data set], https://www.fisheries.noaa.gov/inport/item/48373, 2017.

Orr, D. W. and Ogden, J. C.: The impact of Hurricane Andrew on the ecosystems of South Florida, Conserv. Biol., 6, 488–490, doi:10.1046/j.1523-1739.1992.06040488.x, 1992.

980   Patriquin, D. G.: "Migration" of blowouts in seagrass beds at Barbados and Carriacou, West Indies, and its ecological and geological implications, Aquat. Bot., 1, 163–189, https:// doi. org/ 10. 1016/ 0304-3770(75) 90021-2, 1975.

Patterson, K. L., Porter, J. W., Ritchie, K. B., Poison, S. W., Mueller, E., Peters, E. C., Santavy, D. L., and Smith, G. W.: The etiology of white pox, a lethal disease of the Caribbean elkhorn coral, Acropora palmata, Proc. Natl. Acad. Sci. USA, 99,

985   8725–8730, doi:10.1073/pnas.092260099, 2002.

Perkins, R. D. and Enos, P.: Hurricane Betsy in the Florida-Bahama area: geologic effects and comparison with hurricane Donna, J. Geol., 76, 710–717, https://doi.org/10.1086/627394, 1968.

990   Porter, J. W., Dustan, P., Jaap, W. C., Patterson, K. L., Kosmynin, V., Meier, O. W., Patterson, M. E., and Parsons, M.: Patterns of spread of coral disease in the Florida Keys, Hydrobiologia, 460, 1–24, doi:10.1007/978-94-017-3284-0_1, 2001.

Randall, C., and van Woesik, R.: Contemporary white-band disease in Caribbean corals driven by climate change. Nature Clim. Change 5, 375–379, https://doi.org/10.1038/nclimate2530, 2015.

995

Riazi, A., Vila-Concejo, A., Salles, T., and Türker, U.: Improved drag coefficient and settling velocity for carbonate sands, Sci. Rep. 10, 9465, https://doi.org/10.1038/s41598-020-65741-3, 2020.

Rice, M. M., Ezzat, L., and Burkepile, D. E.: Corallivory in the Anthropocene: interactive effects of anthropogenic stressors

1000   and corallivory on coral reefs, Front. Mar. Sci., 5, 525, doi:10.3389/fmars.2018.00525, 2019.

Rogers, C.S.: Responses of coral reefs and reef organisms to sedimentation, Mar. Ecol. Prog. Ser., 62, 185–202, https://doi.org/10.3354/meps062185, 1990.

1005   Ruzicka, R. R., Colella, M. A., Porter, J. W., Morrison, J. M., Kidney, J. A., Brinkhuis, V., Lunz, K. S., Macaulay, K. A., Bartlett, L. A., Meyers, M. K., and Colee, J.: Temporal changes in benthic assemblages on Florida Keys reefs 11 years after the 1997/1998 El Niño, Mar. Ecol. Prog. Ser., 489, 125–141, doi:10.3354/meps10427, 2013.

Schmoker, J. W. and Halley, R. B.: Carbonate porosity versus depth: a predictable relation for South Florida, AAPG Bull.,

1010   66, 2561–2570, https://doi.org/10.1306/03B5AC73-16D1-11D7-8645000102C1865D, 1982.

Simmons, K. R.; Bohnenstiehl, D. R.; Eggleston, D. B.: Spatiotemporal Variation in Coral Assemblages and Reef Habitat Complexity among Shallow Fore-Reef Sites in the Florida Keys National Marine Sanctuary, Diversity, 14, 153, https://doi.org/10.3390/d14030153, 2022.

1015

Soto, I. M., Muller Karger, F. E., Hallock, P., and Hu, C.: Sea surface temperature variability in the Florida Keys and its relationship to coral cover, J. Mar. Biol., 2011, article ID 981723, doi:10.1155/2011/981723, 2011.

Storlazzi, C. D., Reguero, B. G., Yates, K. K., Cumming, K. A., Cole, A. D., Shope, J. B., Gaido, L., C., Zawada, D. G.,

1020   Arsenault, S. R., Fehr, Z. W., Nickel, B. A., and Beck, M. W.: Rigorously valuing the impact of projected coral reef degradation on coastal hazard risk in Florida, USGS Open-File Report, 2021-1055, 38 pp., doi:10.3133/ofr20211055, 2021.

Takesue, R. K., Sherman, C., Ramirez, N. I., Reyes, A. O., Cheriton, O. M., Rios, R. V., Storlazzi, C. D.: Land-based sediment sources and transport to southwest Puerto Rico coral reefs after Hurricane Maria, May 2017 to June 2018, Estuar.

1025   Coast. Shelf S., 259, 1-12, https://doi.org/10.1016/j.ecss.2021.107476, 2021.

Tilmant, J. T., Curry, R. W., Jones, R. D., Szmant, A., Zieman, J. C., Flora, M., Robblee, M. B., Smith, D., Snow, R. W., and Wanless, H.: Hurricane Andrew's effect on marine resources, BioScience, 44, 230–237, https://doi.org/10.2307/1312227, 1994.

1030

Tonina, D., McKean, J.A., Benjankar, R.M., Wright, C.W., Goode, J.R., Chen, Q., Reeder, W.J., Carmichael, R.A., and Edmondson, M.R.: Mapping river bathymetries: evaluating topobathymetric LiDAR survey, Earth Surf. Process. Landf., 44, 507–520, https://onlinelibrary.wiley.com/doi/10.1002/esp.4513, 2019.

1035   Torres-Garcia, L. M., Dalyander, P. S., Long, J. W., Zawada, D. G., Yates, K. K., Moore, C., & Olabarrieta, M.: Hydrodynamics and sediment mobility processes over a degraded senile coral reef, J. Geophys. Res-Oceans., 123, 7053–7066, https://doi.org/10.1029/2018JC013892, 2018.

Towle, E., Geiger E., Grove, J., Groves, S., Viehman, S., Johnson, M., Blondeau, J., Stein, J., Gorstein, M., Borque, A.,
1040   Acosta, A., Johnson, M., et al.: Coral reef condition: a status report for Florida's Coral Reef, NOAA Coral Reef Conservation Program and the University of Maryland Center for Environmental Science, https://www.coris.noaa.gov/monitoring/status_report/docs/FL_508_compliant.pdf, 2020.

van Woesick, R., Ripple, K., and Miller, S. L.: Macroalgae reduces survival of nursery-reared Acropora corals in the Florida
1045   reef tract, Restor. Ecol., 26, 563–569, doi: 10.1111/rec.12590, 2017.

Viehman, S., Gittings, S., Groves, S., Moore, J., Moore, T., and Stein, J.: NCCOS Assessment: Coral Disturbance Response Monitoring (DRM) along the Florida Reef Tract Following Hurricane Irma from 2017-10-09 to 2017-10-18 (NCEI Accession 0179071), NOAA National Centers for Environmental Information [data set], https://doi.org/10.25921/sscd-6h41, 2018.

1050

Walker, B.: Southeast Florida reef-wide Post-Irma coral disease surveys, Florida Department of Environmental Protection, 37 pp., https://floridadep.gov/sites/default/files/Southeast-Florida-Reef-Wide-Post-Irma-Coral-Disease-Surveys_0.pdf, 2018.

Walter, L. M., Ku, T. C. W., Muehlenbachs, K., Patterson, W. P., and Bonnell, L.: Controls on the $\delta 13C$ of dissolved
1055   inorganic carbon in marine pore waters: an integrated case study of isotope exchange during syndepositional recrystallization of biogenic carbonate sediments (South Florida Platform, USA), Deep-Sea Res. Pt. II, 54, 1163–1200, https://doi.org/10.1016/j.dsr2.2007.04.014, 2007.

Walton, C., Hayes, N. K., and Gilliam, D. S.: Impacts of a regional, multi-year, multi-species coral disease outbreak in
1060   southeast Florida, Front. Mar. Sci., 5, 323, doi:10.3389/fmars.2018.00323, 2018.

Warner, J. C., Armstrong, B., He, R., and Zambon, J. B.: Development of a Coupled Ocean-Atmsophere-Wave-Sediment Transport (COAWST) Modeling System, Ocean Model., 35, 230–244, https://doi.org/10.1016/j.ocemod.2010.07.010, 2010.

1065 Williams, D., and Miller, M.: Attributing mortality among drivers of population decline in *Acropora palmata* in the Florida Keys (USA), Coral Reefs, 31, 369–382, doi: 10.1007/s00338-011-0847-y, 2012.

Wilkinson, C. R.: Global change and coral reefs: impacts on reefs, economies and human culture, Glob. Change Biol., 2, 547–558, doi:10.1111/j.1365-2486.1996.tb00066.x, 1996.

1070

Wilson, S. S., Furman, B. T., Hall, M. O., Fourqurean, J. W.: Assessments of Hurricane Irma impacts on South Florida seagrass communities using long-term monitoring programs, Estuar. Coasts, 43, 1119–1132, https://doi.org/10.1007/s12237-019-00623-0, 2020.

1075 Xian, S., Feng, K., Lin, N., Marsooli, R., Chavas, D., Chen, J., and Hatzikyriakou, A.: Brief communication: Rapid assessment of damaged residential buildings in the Florida Keys after Hurricane Irma, Nat. Hazards Earth Sys., 18, 2041–2045, https://doi.org/10.5194/nhess-18-2041-2018, 2018.

Yates, K. K., Arsenault, S. R., Fehr, Z. W., and Murphy, K. A.: Seafloor elevation change from the 1930s to 2016 along the 1080 Florida Reef Tract, USA, U. S. Geological Survey data release, USGS [data set], https://doi.org/10.5066/P9NXNX61, 2021.

Yates, K. K., Zawada, D. G., Smiley, N. A., and Tiling-Range, G.: Divergence of seafloor elevation and sea level rise in coral reef ecosystems, Biogosciences, 14(6), 1739–1772, doi:10.5194/bg-14-1739-2017, 2017.

1085 Yates, K.K., Zawada, D. G., and Arsenault, S.R.: Seafloor elevation change from 2016 to 2017 at Looe Key, Florida Keys—Impacts from Hurricane Irma (ver. 2.0, November 2020), U.S. Geological Survey data release, USGS [data set], https://doi.org/10.5066/P937LNZF, 2019a.

Yates, K. K., Zawada, D. G., Murphy, K. A., and Arsenault, S. R.: Seafloor elevation change from 2004 to 2016 at Looe Key, 1090 Florida Keys, U.S. Geological Survey data release, USGS [data set], https://doi.org/10.5066/P9JTOOMB, 2019b.

Yoshida, K., Kajikawa, Y., Nishiyama, S., Islam, M.T., Adachi, S., and Sakai, K.: Three-dimensional numerical modelling of floods in river corridor with complex vegetation quantified using airborne LiDAR imagery, J. Hydraul. Res., 1–21, https://www.tandfonline.com/doi/full/10.1080/00221686.2022.2106596, 2022.

1095

Zieg, J. A. and Zawada, D. G.: Seafloor Elevation Change Analysis Tool, U. S. Geological Survey software release, USGS [code], doi: 10.5066/P9D5UUZ0, 2021.

Zitello, A. G., Bauer, L. J., Battista, T. A., Mueller, P. W., Kendall, M. S., and Monaco, M. E.: Shallow-water benthic
1100   habitats of St. John, U.S. Virgin Islands, NOAA technical memorandum NOS NCCOS, 96, 53 pp.